

MARS: Message Passing for Antenna and RF Chain Selection for Hybrid Beamforming in MIMO Communication Systems

Li-Hsiang Shen, Yen-Chun Lo, Kai-Ten Feng, Sau-Hsuan Wu, and Lie-Liang Yang[†]

Department of Electronics and Electrical Engineering,
National Yang Ming Chiao Tung University, Hsinchu, Taiwan

[†]Department of Electronics and Computer Science

University of Southampton, Southampton SO17 1BJ, U.K.

gp3xu4vu6.cm04g@nctu.edu.tw, tommylo0915@gmail.com, ktfeng@nycu.edu.tw,
sauhsuan@nctu.edu.tw, and lly@ecs.soton.ac.uk

Abstract

In this paper, we consider a prospective receiving hybrid beamforming structure consisting of several radio frequency (RF) chains and abundant antenna elements in multi-input multi-output (MIMO) systems. Due to conventional costly full connections, we design an enhanced partially-connected beamformer employing low-density parity-check (LDPC) based structure. As a benefit of LDPC-based structure, information can be exchanged among clustered RF/antenna groups, which results in a low computational complexity order. Advanced message passing (MP) capable of inferring and transferring information among different paths is designed to support LDPC-based hybrid beamformer. We propose a message passing enhanced antenna and RF chain selection (MARS) scheme to minimize the operational power of antennas and RF chains of the receiver. Furthermore, sequential and parallel MP for MARS are respectively designed as MARS-S and MARS-P schemes to address convergence speed issue. Simulations have validated the convergence of both the MARS-P and the MARS-S algorithms. Owing to asynchronous information transfer of MARS-P, it reveals that higher power is required than that of MARS-S, which strikes a compelling balance between power consumption, convergence, and computational complexity. It is also demonstrated that the proposed MARS scheme outperforms the existing benchmarks using heuristic method of fully-/partially-connected architectures in open literature in terms of the lowest power and highest energy efficiency.

Index Terms

Hybrid beamforming, MIMO, LDPC-based connection, antenna selection, RF chain selection, message passing, power consumption, energy efficiency.

I. INTRODUCTION

Wireless communication systems are experiencing revolutionary advances due to rapid changes which the human society creates and shares diverse information. There emerge abundant applications requiring exponentially high wireless traffic demands [1], [2]. In recent years, researchers are investigating promising technology for supporting advanced wireless communication systems with respect to high spectrum and energy efficiency (EE). A denser deployment of base stations (BSs) with larger bandwidth can achieve high performance with increasing degrees of freedom from the perspective of hardware and radio resources but provokes substantial consumption of electricity [3]. Accordingly, serious atmospheric pollution issue will arise due to global carbon emissions ascribed by information and communications technology industry. Therefore, it would be beneficial once BSs are capable of efficiently employing low-power configuration to sustain stringent service requirements as well as resiliently improve the network performance [4].

As a prospect of wireless transmission system, massive multi-input multi-output (MIMO) deployed within a BS is capable of transceiving enormous radio frequency (RF) signals, which is benefited by its gains from multiplexing and diversity [5]. However, it potentially provokes power dissipation in MIMO due to diverse transmission directions. Therefore, beamformer architecture of MIMO should be well-established and appropriately designed in order to concentrate transmission power in certain directions [6]. Conventionally, there exist low-cost analog and high-performance digital beamforming techniques which can resolve the above-mentioned issues [7]. The analog beamforming aims at adjusting the phase shifters of antennas to perform directional data transfer while consuming little circuit power resources. However, limited selection of directional beams are intrinsically induced by the quantized phases from hardware constraints. On the other hand, digital beamforming can perform a more comprehensive task in terms of baseband inter-beam interference cancellation providing full management of directional beam coverage. Nevertheless, digital structure fundamentally requires a variety of RF chains connected to individual antennas, which requires substantial expenditure of configuration, power consumption and transceiver deployment. Therefore, hybrid beamforming (HBF) architecture becomes a promising and implementable solution by leveraging both advantages of low-cost analog structure and highly-directional

digital one [8]. Accordingly, fewer RF chains can be constructed to associate with enormous antennas which reduce cost while sustaining asymptotic performance of digital beamforming.

In recent years, abundant researches focus on architecture designs of HBF but confined to specific structures, i.e., full-connection and sub-connection using separate sub-arrays [9], [10]. Owing to the high degree of freedom of full-connection in HBF, it enables the BS to achieve a nearly optimal solution. In papers [11], they only consider analog beamforming, i.e., beam directions, which aims at maximizing multi-device based resource utilizations. However, joint baseband digital and analog phase shifter precoders should be designed which requires a considerably high computational complexity [12]. In [13], [14], the papers design beamforming schemes from protocol perspectives. Although deep learning can alleviate the complexity issue, it cannot derive either closed-forms or proofs of optimality and convergence [15]. Accordingly, some papers focus on designs of a disjoint solution of analog and digital beamforming under the conventional fully-connected HBF architecture [16], [17]. As for separate sub-arrays in HBF, RF chains take control of independent subsets of phase shifters and antenna elements. From surveys of [9], [10], the authors have investigated a bunch of sub-connection architectures of HBF. In [18], the authors design a disjoint analog/digital beamforming for sub-array architecture. Nonetheless, the performance of sub-arrays is potentially limited due to its inflexibility and inaccessibility of information from other RF chains or antenna sets. The work of [19] minimizes the bit error rate under various RF/antenna connections. Therefore, it becomes compellingly important to design a novel architecture of HBF in order to achieve the benefits of high operational flexibility and asymptotic performance of digital beamforming.

However, with increasingly large-scale HBF with enormous antennas and RF chains serving multiple devices, it will lead to substantially-high overhead in terms of power and complexity, which almost has not been discussed and optimized in the above-mentioned works of [11]–[19]. In [20], the authors discuss about different RF connections for sub-array based HBF. It also observes the power consumption factor under the architectures. In [21], a generalized sub-array-connected architecture is introduced for improving the EE in HBF, which aims at rate optimization problems with each of sub-problem related to a single sub-array. A dynamic adjustment of sub-array architecture under partial-connection is designed to achieve high EE performance [21]. In [22]–[25], the authors address the importance of optimizing EE from either architecture or hardware perspective. The operating power amplifiers and transmit power are considered in [22], [23] but without considerations of RF/antenna effects which are taken into account in [24], [25]. However, they all focus on fully-connected HBF optimizing EE which requires high

complexity. Moreover, under such architecture, it is unnecessary for all RF chains and antennas to be operated owing to worse channel conditions and high power consumption, which should be appropriately selected to prevent performance degradation. The paper of [26] designs antenna selection methods for full-connection HBF maximizing overall data rate. On the other hand, both works of [27], [28] perform RF chain selection in fully-connected HBF by optimizing energy utilizations. However, none of them consider joint selection of RF chains and antennas which is capable of supporting potentially resilient beamforming with high EE. Accordingly, joint design of RF/antenna selection and power consumption as well as flexible architecture of HBF should be considered.

Under the flexible structure of HBF, RF chains are partially connected to the corresponding antenna sets. However, some direct links between RF chains and antennas do not exist which potentially induces vanished information. Message passing (MP) originated from factor graph theory [29] is deemed to be a prospective technique for large-scale networking, which possesses the capability to transfer desirable data¹ and information among enormous links and nodes [30], [31]. In [32], MP-aided sub-array based link optimization is resolved, whereas power allocation problem for beamforming is considered via MP in [33]. The work of [34] designs MP-based receiving beamforming under full-connection; while antenna selection using MP is conceived in [35]. However, joint design of partially-connected HBF and RF/antenna selection has not been studied in previous works. Benefited from resilient HBF, MP is particularly suitable for partially-connected HBF with indirect links. The policy and determination of RF sets can be readily passed through HBF links to the corresponding antenna sets. However, under flexible HBF connection architecture, partial links potentially lead to unreachable information between faraway nodes, which becomes compellingly imperative to design a novel HBF architecture. Inspired by the concept of low-density parity-check (LDPC) [36] coding, it is redesigned and adopted to HBF architecture which ensures that different sets become dependant with the fewest links [37]. In other words, information can be definitely conveyed from one set to the other within polynomial time, which is not considered in existing HBF architecture design. Moreover, under the partial connection of LDPC, MP can effectively and efficiently convey policies among RF/antenna nodes in HBF. Accordingly, we will design a novel flexible HBF architecture by employing LDPC-based structure considering the minimization of power consumption and RF/antenna selection in a massive MIMO communication

¹Note that the term "data" in MP is originated from the field of computer science, which in this paper is referred to as the candidate solution of parameters in our system, i.e., parameters of RF/antenna selections are passed among neighboring nodes. The term data in wireless communication domain specifically indicates transferred "downlink data" resulting in corresponding downlink data rate, which is conveyed from a transmitter and received by a receiver end.

system. Our contributions of this work are summarized as follows.

- We conceive an LDPC-based connection for HBF structure considering antenna and RF chain selection at receiver. Comparing with the fully-connected beamformer, each RF chain is partially connected to a cluster of antennas, which reduces the hardware cost of phase shifters. For arbitrary pairs of RF chains or antennas, we have proven that there exists at least one path which can transfer information from one set to the other within polynomial time, i.e., all RF/antenna sets at receiver are dependant based on LDPC-based connection, which is not revealed in existing partially-connected beamformers.
- We simultaneously consider both antenna and RF chain selections at receiver, which have not been jointly designed in the existing literature. We aim for minimizing the receiver power consumption constrained by minimum transmission data rate and the maximum tolerable system power usage. The formulated problem is decomposed into a pair of sub-problems considering the selection of antennas and RF chains at receiver, respectively, which are computed separately in each virtual processing controller depending on exchanged message.
- We propose a message passing enhanced antenna and RF chain selection (MARS) scheme to minimize the operational circuit power of antennas and RF chains of receiving HBF. Sequential and parallel MP for MARS are designed as MARS-S and MARS-P, respectively. The antenna/RF virtual controller employing MARS-S will pass the determined solutions in a sequential manner, whilst candidate outcomes of MARS-P are simultaneously transmitted to neighboring RF/antenna nodes. Considering computational complexity and convergence issues, MARS can be iteratively performed by either a centralized or distributed manner. A centralized architecture means that more RF/antenna nodes are clustered and managed by an RF/antenna virtual controller, and vice versa for a distributed system.
- We evaluate the system performance of proposed MARS scheme employing LDPC-based connection in receiving HBF under both centralized and distributed architectures. We quantify the power consumption and corresponding EE with respect to different quality-of-service (QoS), numbers of clustered RF/antenna nodes and connections, and insertion loss between RF chains and antenna elements. The proposed MARS outperforms existing techniques in terms of lower power consumption and higher EE.

Notations: We define bold capital letter \mathbf{A} as a matrix, bold lowercase letter \mathbf{a} as a vector, and \mathcal{A} as a set. $[\mathbf{A}]_{mn}$ denotes the (m, n) -th element of matrix \mathbf{A} . Matrix operations of \mathbf{A}^H and \mathbf{A}^{-1} represent

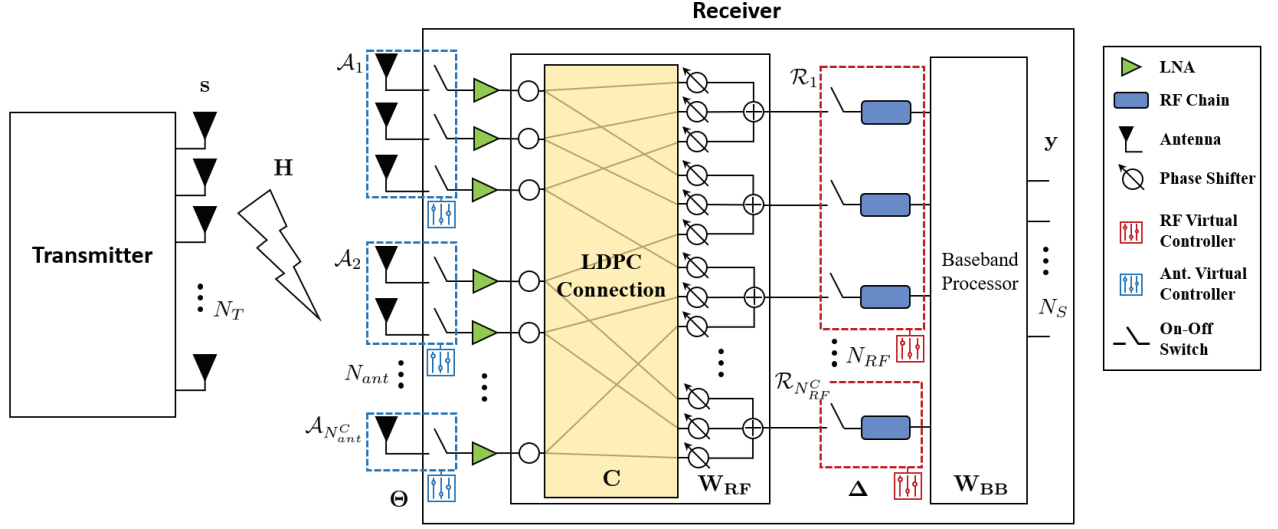


Fig. 1. Proposed structure of downlink antenna and RF chain selection for hybrid beamforming.

Hermitian transpose and inverse of \mathbf{A} . $\det(\cdot)$, $\text{diag}(\cdot)$ and $\mathbb{E}[\cdot]$ are defined as the determinant, diagonal matrix and expectation operation, respectively. $\mathbb{1}(\mathcal{X})$ denotes an indicator function which is one when event \mathcal{X} takes place. The operations of \neg , \wedge , \vee and \oplus indicate the binary-wise logical operations of NOT, AND, OR and Exclusive-OR, respectively. Also, \bigvee denotes the sequential logic operations of \vee , i.e., $\bigvee_{i=1}^{N_x} x_i = x_1 \vee x_2 \dots \vee x_{N_x}$, where N_x is the dimension of $\{x_i\}$. $\text{mod}(a, b)$ is the module operation with arbitrary integer a and b , e.g., $\text{mod}(a, b) = 0$ indicates that a is an integer multiple of b . $\lceil \cdot \rceil$ is a ceiling function.

II. SYSTEM MODEL AND PROBLEM FORMULATION

A. System Model

We consider a partially-connected HBF architecture at receiving BS in a downlink massive MIMO communication system as shown in Fig. 1. The receiving BS is equipped with RF chains $\mathcal{R} \in \{1, \dots, n, \dots, N_{RF}\}$ and antenna elements $\mathcal{A} \in \{1, \dots, m, \dots, N_{ant}\}$, where N_{RF} and N_{ant} indicate the total number of HBF RF chains and antennas, respectively. Without loss of generality, we assume that the hybrid beamformer possesses fewer RF chains than antennas due to reduction of hardware expenditure in fully-digital beamformer, i.e., $N_{RF} \leq N_{ant}$. The receiving HBF consists of analog beamformer $\mathbf{W}_{RF} \in \mathbb{C}^{N_{RF} \times N_{ant}}$ and baseband digital beamformer $\mathbf{W}_{BB} \in \mathbb{C}^{N_S \times N_{RF}}$, where N_S denotes the number of received data streams. Note that the connection $\mathbf{C} \in \mathbb{Z}^{N_{RF} \times N_{ant}}$ between the analog and baseband beamformers can be

either in fully-connected or partially-connected manner, where $[\mathbf{C}]_{nm} \in \{0, 1\}, \forall n, m$, indicates whether the n -th RF chain is linked to the m -th antenna. The desired transmitted signal is defined as $\mathbf{s} \in \mathbb{C}^{N_T \times 1}$, where N_T is the number of antennas at transmit BS. Note that \mathbf{s} is the final beamformed signal at transmitter having the identical number of received data streams N_S .

In order to manage the energy consumption of HBF, we can switch off spoiled RF chains or antennas to optimize the power utilization. The selection matrices of RF chains and antenna elements are respectively denoted as $\mathbf{\Delta} = \text{diag}(\boldsymbol{\delta}) = \text{diag}(\delta_1, \dots, \delta_n, \dots, \delta_{N_{RF}})$ and $\mathbf{\Theta} = \text{diag}(\boldsymbol{\theta}) = \text{diag}(\theta_1, \dots, \theta_m, \dots, \theta_{N_{ant}})$, where $\delta_n \in \{0, 1\}$ and $\theta_m \in \{0, 1\}$ indicate the selection decision of RF chains and antennas, e.g., $\delta_n = 1$ and $\theta_m = 1$ mean that n -th RF chain and m -th antenna are selected to be turned on. Since we focus on the designs at receiver HBF, the transmission power P_T is considered to be equally allocated to transmit antennas², i.e., we have $\mathbb{E}[\mathbf{s}\mathbf{s}^H] = \frac{P_T}{N_T} \mathbf{I}_{N_T}$, where \mathbf{I}_{N_T} is the identity matrix with the size of N_T . The received downlink signal is given by

$$\mathbf{y} = \sqrt{\rho(1-\beta)} \mathbf{W}_{\text{BB}} \mathbf{\Delta} (\mathbf{C} \circ \mathbf{W}_{\text{RF}}) \mathbf{\Theta} \mathbf{H} \mathbf{s} + \mathbf{W}_{\text{BB}} (\mathbf{C} \circ \mathbf{W}_{\text{RF}}) \mathbf{n}, \quad (1)$$

where \circ is Hadamard product for element-wise multiplication. In (1), ρ is the distance-based loss and $\mathbf{H} \in \mathbb{C}^{N_{ant} \times N_T}$ is the small-scale fading channel which is defined based on Saleh Valenzuela model [18], [23] as

$$\mathbf{H} = \sqrt{\frac{N_T N_{ant}}{L}} \sum_{\ell=1}^L \alpha_\ell \cdot \boldsymbol{\alpha}_r(\phi_\ell^r) \boldsymbol{\alpha}_t^H(\phi_\ell^t), \quad (2)$$

where L is the number of multi-paths and $\alpha_\ell \sim \mathcal{CN}(0, 1)$ is complex channel gain of the ℓ -th path. The array response vector corresponding to angle-of-arrival (AoA) of HBF receiver and angle-of-departure (AoD) of the transmit BS are given by $\boldsymbol{\alpha}_r(\phi_\ell^r)$ and $\boldsymbol{\alpha}_t(\phi_\ell^t)$, respectively, along with their incident receiving and transmit angles of ϕ_ℓ^r and ϕ_ℓ^t . In (1), notation $\mathbf{n} \sim \mathcal{CN}(0, N_0 \mathbf{I}_{N_R})$ is complex additive white Gaussian noise with noise power spectral density of N_0 . Furthermore, we consider the insertion loss β in the downlink receiving HBF-based BS [38], which is the connection loss between an RF chain and its connected antenna elements due to signal power dissipation. Based on the received downlink

²Note that \mathbf{s} can be similarly generated with transmit beamforming technique as considered in most of papers, i.e., \mathbf{s} can be demonstrated in a form of $\mathbf{s} = \mathbf{W}_{\text{RF}, \text{tx}} \mathbf{W}_{\text{BB}, \text{tx}} \mathbf{x}$, where $\mathbf{W}_{\text{RF}, \text{tx}}$, $\mathbf{W}_{\text{BB}, \text{tx}}$ and \mathbf{x} are defined as transmit RF, baseband beamformers, and original transmit signal, respectively. However, this will require compellingly complex algorithms with unaffordable complexity order when jointly considering both transmit and receiving beamforming as well as RF/antenna selection mechanisms.

signal in (1), the achievable system rate can be written as

$$R(\mathbf{\Delta}, \mathbf{\Theta}) = \log_2 \left[\det \left(\mathbf{I}_{N_S} + \frac{P_T \rho (1 - \beta)}{N_0 N_T} \mathbf{W}_{BB} \mathbf{\Delta} (\mathbf{C} \circ \mathbf{W}_{RF}) \mathbf{\Theta} \mathbf{H} \mathbf{H}^H \right. \right. \\ \left. \left. \mathbf{\Theta}^H \mathbf{W}_{RF}^H \mathbf{\Delta}^H \mathbf{W}_{BB}^H (\mathbf{W}_{BB} (\mathbf{C} \circ \mathbf{W}_{RF}) \mathbf{W}_{RF}^H \mathbf{W}_{BB}^H)^{-1} \right) \right]. \quad (3)$$

The total power consumption at the receiver HBF-based BS can be represented by [23], [25]

$$P(\boldsymbol{\delta}, \boldsymbol{\theta}) = P_{BB} + \sum_{n=1}^{N_{RF}} \sum_{m=1}^{N_{ant}} [\delta_n (P_{RF} + P_{ADC}) + \theta_m P_{LNA} + [\mathbf{C}]_{nm} \delta_n \theta_m P_{PS}], \quad (4)$$

where P_{BB} , P_{RF} , P_{ADC} , P_{LNA} and P_{PS} denote the circuit power of HBF baseband signal processing, operations of RF chains, analog-to-digital converter, low-noise power amplifiers and phase shifters at receiving antennas, respectively. We can observe that (4) includes static power of P_{BB} and dynamic power terms of P_{RF} , P_{ADC} , P_{LNA} and P_{PS} because the dynamic ones are determined by the selection of RF chains and antennas. The system parameters and corresponding notations are listed in Table I.

B. Problem Formulation

Benefited by the partial HBF architecture that employs LDPC-based connection, the hardware expenditure can be effectively reduced while guaranteeing the dependency of decided information, i.e., information can be exchanged within arbitrary nodes of RF chains and antennas. In this paper, we aim at minimizing the total operational circuit power $P(\boldsymbol{\delta}, \boldsymbol{\theta})$ by selecting the candidate RF chains of $\boldsymbol{\delta}$ and antenna elements of $\boldsymbol{\theta}$ at the downlink receiving HBF-enabled BS, which is given by

$$\min_{\boldsymbol{\delta}, \boldsymbol{\theta}} P(\boldsymbol{\delta}, \boldsymbol{\theta}), \quad (5a)$$

$$\text{s.t. } \delta_n \in \{0, 1\}, \quad \forall n, \quad (5b)$$

$$\theta_m \in \{0, 1\}, \quad \forall m, \quad (5c)$$

$$N_S \leq \sum_{n=1}^{N_{RF}} \delta_n \leq \sum_{m=1}^{N_{ant}} \theta_m, \quad (5d)$$

$$R(\mathbf{\Delta}, \mathbf{\Theta}) \geq R_{req}, \quad (5e)$$

$$P(\boldsymbol{\delta}, \boldsymbol{\theta}) \leq P_{max}, \quad (5f)$$

$$P_{PS} \sum_{m=1}^{N_{ant}} \theta_m [\mathbf{C}]_{nm} \leq (1 - \beta) P_o, \quad \forall n. \quad (5g)$$

TABLE I
DEFINITION OF SYSTEM PARAMETERS

Parameters	Notation
Set of antenna and RF chains	\mathcal{A}, \mathcal{R}
Number of transmit/receiving antennas/RF chains	N_T, N_{ant}, N_{RF}
Number of data streams	N_S
HBF analog and baseband beamformer	$\mathbf{W}_{RF}, \mathbf{W}_{BB}$
HBF connection	\mathbf{C}
Selection matrix of RF/antenna	Δ, Θ
Element-wise selection of RF/antenna	δ_n, θ_m
Transmit/received/noise signal	$\mathbf{s}, \mathbf{y}, \mathbf{n}$
Transmit power	P_T
Noise power	N_0
Small/large scale channel fading	\mathbf{H}, ρ
Antenna gain function	$\Lambda(\phi_\ell)$
Number of multi-paths	L
Insertion loss	β
Achievable rate	$R(\Delta, \Theta)$
Total power consumption	$P(\delta, \theta)$
Power of baseband/RF/LNA/phase shifter	$P_{BB}, P_{RF}, P_{LNA}, P_{PS}$
Number of LDPC connections	N_{Conn}
Set of RF/antenna controllers	$\mathcal{R}^C, \mathcal{A}^C$
The k -th RF/ l -th antenna controller	$\mathcal{R}_k, \mathcal{A}_l$
Number of RF/antenna controllers	N_{RF}^C, N_{ant}^C
Number of RF/antenna elements controlled	$N_{RF,k}, N_{ant,l}$
RF decision/antenna update set of RF controller	$\delta_{\mathcal{R}_k}, \theta_{\mathcal{R}_k,l}$
Antenna decision/RF update set of antenna controller	$\theta_{\mathcal{A}_l}, \delta_{\mathcal{A}_l,k}$
MP operation from RF to antenna controller	$\mu_{\mathcal{R}_k \rightarrow \mathcal{A}_l}(\cdot)$
MP operation from antenna to RF controller	$\nu_{\mathcal{A}_l \rightarrow \mathcal{R}_k}(\cdot)$
Threshold of RF/antenna selection	η_r, η_a

Constraints (5b) and (5c) represent the binary selection decisions of RF chains and antenna elements, respectively. The constraint (5d) indicates the limitation of HBF architecture that the number of data streams is fewer than that of the operating RF chains, whilst the number of selected RF chains is generally smaller than that of the operating antennas. (5e) guarantees the minimum QoS requirement of R_{req} at the downlink HBF-enabled receiving BS. Note that $\{\Delta, \Theta\}$ are the RF/antenna selection matrices for $\{\delta, \theta\}$ which are in vector forms. The constraint (5f) confines the maximum allowable system power defined as P_{max} . In (5g), we consider that each RF chain can supply the maximum output power P_o for antenna elements under the circuit insertion loss β at receiver. Note that we consider random beamforming in problem (5) and optimize the total power consumption since the beamformer designs of \mathbf{W}_{RF} and \mathbf{W}_{BB} will induce an unsolvable problem. It couples the continuous beamformer variables with the RF/antenna selection functions. We can observe from problem (5) that the solution cannot be readily attained due to high computational complexity. Therefore, we conceive an MP-empowered RF/antenna

selection scheme under the LDPC-based HBF connection which is elaborated in the following sections.

III. DESIGN OF LDPC-BASED HBF CONNECTION

Inspired by the parity-check property in coding theory, we conceive a LDPC-based HBF connection \mathbf{C} between RF chains and antennas, which is partially linked with the following properties as [36]

$$\sum_{m=1}^{N_{ant}} [\mathbf{C}]_{nm} = N_{Conn} \stackrel{(a)}{>} \left\lceil \frac{N_{ant}}{N_{RF}} \right\rceil, \quad \forall n, \quad (6a)$$

$$\sum_{n=1}^{N_{RF}} [\mathbf{C}]_{nm} \geq 1, \quad \forall m, \quad (6b)$$

$$\sum_{n=1}^{N_{RF}} \sum_{n'=n+1}^{N_{RF}} \mathbb{1}(\chi_{nn'} \geq 1) \geq N_{RF} - 1, \quad (6c)$$

where N_{Conn} indicates the number of antennas connected to an RF chain, and $\chi_{nn'} = \sum_{m=1}^{N_{ant}} \mathbb{1}([[\mathbf{C}]_{nm} + [\mathbf{C}]_{n'm}] \geq 2)$ denotes the number of commonly-paired antenna nodes. Note that the ceiling operation $\lceil \cdot \rceil$ prevents non-integer values when $\varrho = \text{mod}(N_{ant}, N_{RF}) \neq 0$, and inequality (a) in (6a) guarantees the LDPC property that there exists at least a direct or an indirect link between two arbitrary nodes of RF chains or antennas. It is worth mentioning that constraint (6c) is different from original parity-check mechanism, which ensures interconnection among RF/antenna nodes as proven in the following lemma.

Definition 1. *Given a number of nodes x , we only require $(x-1)$ edges to establish connection among them. The worst case is that nodes 1 and x are capable of communicating via the maximum $(x-1)$ hops, whilst the best case with the minimum distance is a single hop between any of neighboring nodes.*

Lemma 1. *Considering the LDPC-based connection scheme in (6), there exists at least a direct or an indirect link between two arbitrary nodes of RF chains or antennas.*

Proof. We start from $N_{Conn} = \left\lceil \frac{N_{ant}}{N_{RF}} \right\rceil$, which implies that at least independent links can be constructed considering constraint (6b), e.g., $[\mathbf{C}]_{nm} = 1$ when $(n-1) \cdot \left\lceil \frac{N_{ant}}{N_{RF}} \right\rceil + 1 \leq m \leq n \cdot \left\lceil \frac{N_{ant}}{N_{RF}} \right\rceil$. Now, we provide an additional link as $N_{Conn} = \left\lceil \frac{N_{ant}}{N_{RF}} \right\rceil + 1$, which indicates that there will exist $N_{ant} - \left\lceil \frac{N_{ant}}{N_{RF}} \right\rceil$ antenna selection cases. Therefore, according to (6c), given arbitrary two RF chains, they should have at least a single common connected antenna, i.e., $\mathbb{1}([\mathbf{C}]_{nm} + [\mathbf{C}]_{n'm}] \geq 2)$ when $n \neq n'$. Moreover, based on Definition 1 and the last inequality of (6c), we are able to guarantee that there exists at least

a direct or an indirect link between two arbitrary nodes of RF chains or antennas. This completes the proof. \square

From Lemma 1, we can observe from (6) that it reaches higher spatial diversity when N_{Conn} grows and achieves the full connection architecture if $N_{Conn} = N_{ant}$ holds. By contrast, when $N_{Conn} = \left\lceil \frac{N_{ant}}{N_{RF}} \right\rceil$ we have a basic architecture of partially-connected method. Compared to the fully-connected structure of HBF, the designed LDPC-based HBF architecture can reduce the hardware expenditure. Moreover, under the established architecture, all nodes of RF chains and antennas will be dependant according to Lemma 1, i.e., information can be conveyed from one node to another one within finite time. The construction algorithm of the proposed LDPC-based HBF connection³ between RF/antenna is demonstrated in Algorithm 1. In Fig. 2, we have provided an example for construction of proposed LDPC-based structure for MP scheme. As can be seen from Fig. 2(a) following Algorithm 1, we firstly establish $N_{Conn} - 1 = 2$ links (red solid lines) between RF chains and antenna nodes to satisfy (6b), whilst an additional link (blue dotted lines) per RF chain is associated satisfying (6a) for $N_{Conn} = 3$. The constraint (6c) is also guaranteed with $\chi_{12} = 2$, $\chi_{23} = 1$, and $\chi_{13} = 1$, i.e., $\sum_{n=1}^3 \sum_{n'=n+1}^3 \mathbb{1}(\chi_{nn'} \geq 1) = 3$. Therefore, message can be conveyed to arbitrary nodes (green arrows). On the other hand, if the number of antennas is integer multiple of RF chains as exemplified in Fig. 2(b), it will provoke some independent association between arbitrary nodes at first-phase construction. For example, message from antenna 6 cannot be passed to antenna 4 via red paths. To conquer this, additional blue paths obeying (6c) provide connection among arbitrary nodes, e.g., message between antennas 4 and 6 can therefore be perfectly delivered but with more hops.

In order to manage RF chains and antenna elements in the downlink receiving BS, we consider that the HBF architecture is divided into several distributed virtual controllers as RF and antenna controllers. That is, several RF chains and antennas are clustered and controlled by their corresponding controllers, which are depicted in Fig. 1. Note that we use the term controller indicating virtual controller in the remaining content for simplicity. In the LDPC-based connected HBF architecture, we deploy N_{RF}^C RF chain controllers as $\mathcal{R}^C \in \{\mathcal{R}_1, \dots, \mathcal{R}_k, \dots, \mathcal{R}_{N_{RF}^C}\}$ and N_{ant}^C antenna controllers as $\mathcal{A}^C \in \{\mathcal{A}_1, \dots, \mathcal{A}_l, \dots, \mathcal{A}_{N_{ant}^C}\}$, where \mathcal{R}_k and \mathcal{A}_l denote the control units of the k -th RF chain controller and the l -th antenna controller,

³We can implement the proposed LDPC-based connection by initializing a configuration of fully-connected HBF. After obtaining the optimal LDPC connection in Algorithm 1, we are able to permanently turn off those unused links between RF chains and antennas, leaving the remaining elements operable. To elaborate a little further, LDPC connection can be regarded as a longer-term mechanism compared to the short-term element selection dealing with small-scale fading channel. Leveraging such scheme requires a further complex analysis and design, which is out of scope of this paper and can be left as future promising work.

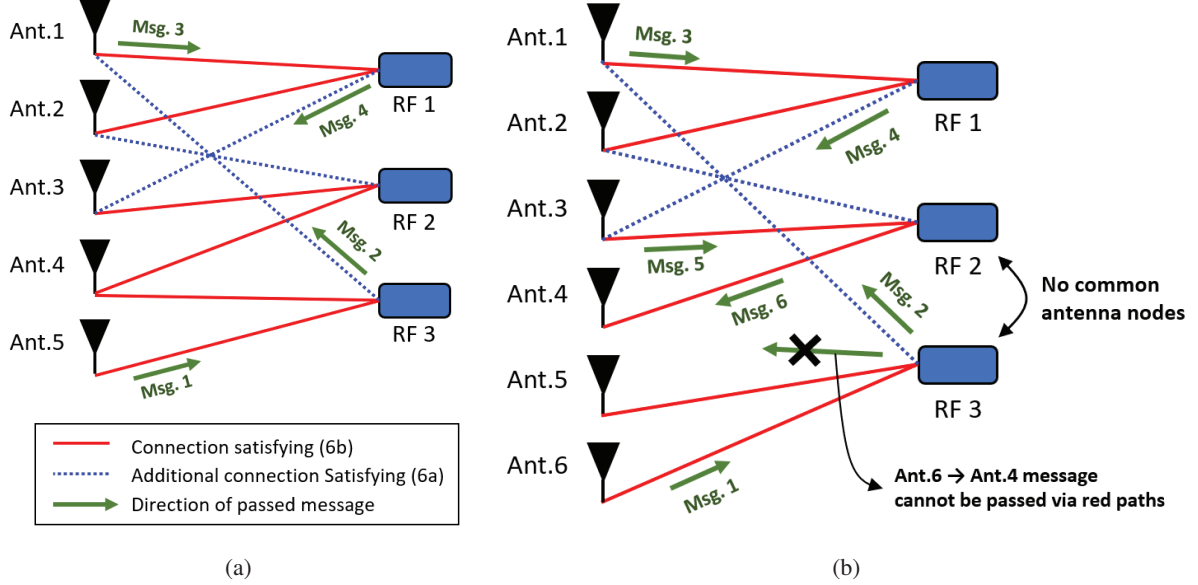


Fig. 2. Example of the proposed LDPC-based structure for MP considering $\varrho = \text{mod}(N_{ant}, N_{RF})$ with $N_{ant} \in \{5, 6\}$ antenna nodes and $N_{RF} = 3$ RF chain nodes. (a) $\varrho \neq 0$ and $N_{ant} = 5$ (b) $\varrho = 0$ and $N_{ant} = 6$. Note that Ant. and Msg. are acronyms of antenna and message, respectively.

respectively. Without loss of generality, antennas and RF chains cannot be managed by more than one controller, i.e., $\mathcal{R}_k \cap \mathcal{R}_{k'} = \emptyset, \forall k' \neq k$, and $\mathcal{A}_l \cap \mathcal{A}_{l'} = \emptyset, \forall l' \neq l$. We consider that RF controller \mathcal{R}_k manages $N_{RF,k}$ RF chains and antenna controller \mathcal{A}_l takes care of $N_{ant,l}$ antenna elements. Owing to the designed partial HBF structure, each control unit only attains partial knowledge from neighboring linked nodes and its own determination. Therefore, we define that the k -th RF chain controller possesses itself RF decision set of $\delta_{\mathcal{R}_k} = \{\delta_{\mathcal{R}_k,1}, \dots, \delta_{\mathcal{R}_k,N_{RF,k}}\}$ and the antenna decision from the l -th connected antenna controller of $\theta_{\mathcal{R}_k,l} = \{\theta_{\mathcal{R}_k,l,1}, \dots, \theta_{\mathcal{R}_k,l,N_{ant,l}}\}$. Similarly, the l -th antenna controller has its own antenna decision set of $\theta_{\mathcal{A}_l} = \{\theta_{\mathcal{A}_l,1}, \dots, \theta_{\mathcal{A}_l,N_{ant,l}}\}$ and RF selection decision from the neighboring RF controller k of $\delta_{\mathcal{A}_l,k} = \{\delta_{\mathcal{A}_l,k,1}, \dots, \delta_{\mathcal{A}_l,k,N_{RF,k}}\}$. Note that the policy subsets at each controller are included in the total set of RF and antenna selections as $\{\delta_{\mathcal{R}_k}, \delta_{\mathcal{A}_l,k}, \forall k, l\} \in \delta$ and $\{\theta_{\mathcal{A}_l}, \theta_{\mathcal{R}_k,l}, \forall k, l\} \in \theta$, respectively.

IV. PROPOSED MESSAGE PASSING ANTENNA AND RF CHAIN SELECTION (MARS) SCHEME

Owing to its high computational complexity, the original problem in (5) is decomposed into two subproblems, i.e., RF chain selection and antenna selection, which are determined by RF and antenna controllers, respectively. For each controller, it will solve for its own solution according to the messages passed from other controllers, which can potentially reduce the system complexity. The sub-problem of

Algorithm 1: LDPC-based HBF connection

```

1: Initialization:  $\mathcal{A}, \mathcal{R}, N_{Conn}$ 
2: (Independent Connection Establishment)
3: Set temporary non-established connection set as  $\mathcal{M} = \mathcal{A}$ 
4: for  $n = 1, \dots, N_{RF}$  do
5:   Randomly select a subset  $\mathcal{M}'$  with  $\left\lceil \frac{N_{ant}}{N_{RF}} \right\rceil$  elements from  $\mathcal{M}$ 
6:   Generate a binary vector indexed by subset  $\mathcal{M}'$  based on (6a), i.e., we have  $[\mathbf{C}]_{nm} = 1$  for  $m \in \mathcal{M}'$  with
     remaining elements as zero for  $m \notin \mathcal{M}'$ 
7:   Update the non-established connection set as  $\mathcal{M} \leftarrow \mathcal{M} - \mathcal{M}'$ 
8: end for
9: (Node Dependency Construction)
10: Randomly select an initial pairing RF candidate  $n \in \mathcal{R}$ 
11: Set temporary non-selected RF set as  $\mathcal{N} = \mathcal{R} \setminus \{n\}$ 
12: for  $iter = 1, \dots, N_{RF} - 1$  do
13:   Randomly select a pairing RF as  $n' \in \mathcal{N} \setminus \{n\}$ 
14:   Choose any common antenna node  $m$  with  $\mathbf{C}_{n'm} = 1$  and set  $\mathbf{C}_{nm} = 1$ 
15:   Update non-selected RF set as  $\mathcal{N} \leftarrow \mathcal{N} \setminus \{n'\}$  and  $n = n'$ 
16: end for

```

RF selection for the k -th RF chain controller is written as

$$\min_{\boldsymbol{\delta}_{\mathcal{R}_k}} P(\boldsymbol{\delta}_{\mathcal{R}_k}) \quad (7a)$$

$$\text{s.t. Fixed } \boldsymbol{\theta}_{\mathcal{R}_k, l}, \boldsymbol{\delta}_{\mathcal{R}_{k'}}, \forall l, k' \neq k, \quad (7b)$$

$$(5b), (5d), (5e), (5f), \quad (7c)$$

where (7a) indicates the power consumption of k -th RF chain given by the passed information of $\boldsymbol{\theta}_{\mathcal{R}_k, l}$ from the l -th antenna controller and the message of $\boldsymbol{\delta}_{\mathcal{R}_{k'}}$ from the neighboring (k')-th RF chain in (7b).

Furthermore, the sub-problem of antenna selection for the l -th RF chain controller is given by

$$\min_{\boldsymbol{\theta}_{\mathcal{A}_l}} P(\boldsymbol{\theta}_{\mathcal{A}_l}) \quad (8a)$$

$$\text{s.t. Fixed } \boldsymbol{\delta}_{\mathcal{A}_l, k}, \boldsymbol{\theta}_{\mathcal{A}_{l'}}, \forall k, l' \neq l, \quad (8b)$$

$$(5c), (5d), (5e), (5f), (5g), \quad (8c)$$

where (8a) represents the total power consumption of l -th antenna controller given by the passed information of $\boldsymbol{\delta}_{\mathcal{A}_l, k}$ from the k -th RF controller and the message of $\boldsymbol{\theta}_{\mathcal{A}_{l'}}$ from the neighboring (l')-th antenna controller in (8b). To deal with the two sub-problems of RF/antenna selection, we propose MARS scheme to minimize the operational circuit power of antennas and RF chains of receiving HBF.

Two types of MARS are designed as the sequential and parallel message passing, correspondingly denoted as MARS-S and MARS-P, respectively. Note that MARS can be iteratively performed by either a centralized or distributed manner based on the considerations of computational complexity and algorithm convergence. The centralized architecture indicates that more RF/antenna nodes are managed by an RF/antenna controller, and vice versa for a distributed system. In the following, we will elaborate the MARS scheme in terms of MARS-S and MARS-P.

A. MARS-S of Sequential Message Passing

In the proposed sequential mechanism of MARS-S, the antenna/RF controller will pass the determined solutions in a sequential manner. As a result, the controllers are guaranteed to acquire the latest information from their neighboring nodes. The overall procedure of MARS-S is shown in Fig. 3, including four parts of processing which are elaborated in the followings.

1) *Initialization*: At the beginning, all RF chain and antenna controllers will exchange the determined beamformer matrices of \mathbf{W}_{BB} and \mathbf{W}_{RF} and channel information \mathbf{H} in order to compute the achievable rate in (3). Furthermore, all RF/antenna selection elements in δ and θ are randomly generated in $\{0, 1\}$.

2) *Update from Received Message*: Afterwards, the RF/antenna controllers will update its latest information of RF/antenna selections based on the received message from the neighboring controllers. According to (7a), the update information of the k -th RF chain controller at the t -th update consists of the (k') -th RF chain decision $\delta_{\mathcal{R}_{k'}}, \forall k' \neq k$ and the passed antenna selection $\theta_{\mathcal{R}_k, l}, \forall l$ at the $(t-1)$ -th iteration, which are given by

$$\delta_{\mathcal{R}_{k'}}^{(t)} = \bigvee_{\mathcal{A}_l \in \mathcal{C}_{\mathcal{R}_k}} \left[\Xi_{\mathcal{R}} \wedge \nu_{\mathcal{A}_l \rightarrow \mathcal{R}_k} \left(\delta_{\mathcal{A}_l, k'}^{(t-1)} \right) \right] \wedge \left\{ \neg \left[\bigvee_{\mathcal{A}_l \in \mathcal{C}_{\mathcal{R}_k}} \left(\Xi_{\mathcal{R}} \wedge \delta_{\mathcal{R}_{k'}}^{(t-1)} \right) \right] \right\}, \quad (9a)$$

$$\theta_{\mathcal{R}_k, l}^{(t)} = \bigvee_{\mathcal{A}_l \in \mathcal{C}_{\mathcal{R}_k}} \left[\Xi'_{\mathcal{R}} \wedge \nu_{\mathcal{A}_l \rightarrow \mathcal{R}_k} \left(\theta_{\mathcal{A}_l}^{(t-1)} \right) \right] \wedge \left\{ \neg \left[\bigvee_{\mathcal{A}_l \in \mathcal{C}_{\mathcal{R}_k}} \left(\Xi'_{\mathcal{R}} \wedge \theta_{\mathcal{R}_k, l}^{(t-1)} \right) \right] \right\}, \quad (9b)$$

where $\Xi_{\mathcal{R}} = \nu_{\mathcal{A}_l \rightarrow \mathcal{R}_k} \left(\delta_{\mathcal{A}_l, k'}^{(t-1)} \right) \oplus \delta_{\mathcal{R}_{k'}}^{(t-1)}$ and $\Xi'_{\mathcal{R}} = \nu_{\mathcal{A}_l \rightarrow \mathcal{R}_k} \left(\theta_{\mathcal{A}_l}^{(t-1)} \right) \oplus \theta_{\mathcal{R}_k, l}^{(t-1)}$. The connection set of the k -th RF controller linked to its antenna controllers is denoted as $\mathcal{C}_{\mathcal{R}_k}$. Furthermore, we define $\nu_{\mathcal{A}_l \rightarrow \mathcal{R}_k}(\cdot)$ as the message passing operation which directs the path from the l -th antenna controller to the k -th RF chain controller. Similarly, according to (8a), the message of the l -th antenna controller at the t -th update consists of the (l') -th antenna selection $\theta_{\mathcal{A}_{l'}}, \forall l' \neq l$ and the passed RF policy $\delta_{\mathcal{A}_l, k}, \forall k$ at the

$(t - 1)$ -th iteration, which are obtained as

$$\boldsymbol{\theta}_{\mathcal{A}_{l'}}^{(t)} = \bigvee_{\mathcal{R}_k \in \mathcal{C}_{\mathcal{A}_l}} \left[\Xi_{\mathcal{A}} \wedge \mu_{\mathcal{R}_k \rightarrow \mathcal{A}_l} \left(\boldsymbol{\theta}_{\mathcal{R}_k, l'}^{(t-1)} \right) \right] \wedge \left\{ \neg \left[\bigvee_{\mathcal{R}_k \in \mathcal{C}_{\mathcal{A}_l}} \left(\Xi_{\mathcal{A}} \wedge \boldsymbol{\theta}_{\mathcal{A}_{l'}}^{(t-1)} \right) \right] \right\}, \quad (10a)$$

$$\boldsymbol{\delta}_{\mathcal{A}_{l,k}}^{(t)} = \bigvee_{\mathcal{R}_k \in \mathcal{C}_{\mathcal{A}_l}} \left[\Xi'_{\mathcal{A}} \wedge \mu_{\mathcal{R}_k \rightarrow \mathcal{A}_l} \left(\boldsymbol{\delta}_{\mathcal{R}_k}^{(t-1)} \right) \right] \wedge \left\{ \neg \left[\bigvee_{\mathcal{R}_k \in \mathcal{C}_{\mathcal{A}_l}} \left(\Xi'_{\mathcal{A}} \wedge \boldsymbol{\delta}_{\mathcal{A}_{l,k}}^{(t-1)} \right) \right] \right\}, \quad (10b)$$

where $\Xi_{\mathcal{A}} = \mu_{\mathcal{R}_k \rightarrow \mathcal{A}_l} \left(\boldsymbol{\theta}_{\mathcal{R}_k, l'}^{(t-1)} \right) \oplus \boldsymbol{\theta}_{\mathcal{A}_{l'}}^{(t-1)}$ and $\Xi'_{\mathcal{A}} = \mu_{\mathcal{R}_k \rightarrow \mathcal{A}_l} \left(\boldsymbol{\delta}_{\mathcal{R}_k}^{(t-1)} \right) \oplus \boldsymbol{\delta}_{\mathcal{A}_{l,k}}^{(t-1)}$. Notation $\mathcal{C}_{\mathcal{A}_l}$ indicates the connection set of the l -th antenna controller associated with its RF controllers. Moreover, $\mu_{\mathcal{R}_k \rightarrow \mathcal{A}_l}(\cdot)$ is defined as the message passing operation directing the path from the k -th RF controller to the l -th antenna controller. Benefited by MP mechanism, we can observe from the update equations of (9) and (10) that the RF/antenna controllers can readily update all information of the other RF/antenna nodes via simple logic operations in order to achieve their optimal solution of RF/antenna selections.

3) *Optimization*: Based on (9) and (10), the RF/antenna controllers will solve the decomposed subproblems in (7) and (8) to obtain the optimum of RF chain and antenna selections which are given by

$$\boldsymbol{\delta}_{\mathcal{R}_k}^* = \operatorname{argmin}_{\boldsymbol{\delta}_{\mathcal{R}_k}} P(\boldsymbol{\delta}_{\mathcal{R}_k}) \text{ with fixed } \boldsymbol{\theta}_{\mathcal{R}_k, l}, \boldsymbol{\delta}_{\mathcal{R}_{k'}}, \forall l, k' \neq k, \quad (11)$$

and

$$\boldsymbol{\theta}_{\mathcal{A}_l}^* = \operatorname{argmin}_{\boldsymbol{\theta}_{\mathcal{A}_l}} P(\boldsymbol{\theta}_{\mathcal{A}_l}) \text{ with fixed } \boldsymbol{\delta}_{\mathcal{A}_{l,k}}, \boldsymbol{\theta}_{\mathcal{A}_{l'}}, \forall k, l' \neq l, \quad (12)$$

respectively. Note that all constraints of RF/antenna should be obeyed in (7c) and (8c), respectively. Due to the partial connection of LDPC-based HBF architecture, each controller is capable of managing a small number of nodes, which can achieve a much lower complexity. Accordingly, we can readily employ a numerical brute-force method for obtaining the optimal binary-based parameters, i.e., we search all possible solutions for a group of nodes given the passed information from others. Therefore, each RF/antenna controller can obtain their respective optimal solutions of RF selection in (11) and antenna selection in (12).

4) *Sequential Passing Message*: After obtaining the optimal outcome of RF/antenna selection, the first controller will pass its latest information to the neighboring connected nodes based on the LDPC-based HBF architecture. Then, the second controller managing its RF chains or antennas will determine

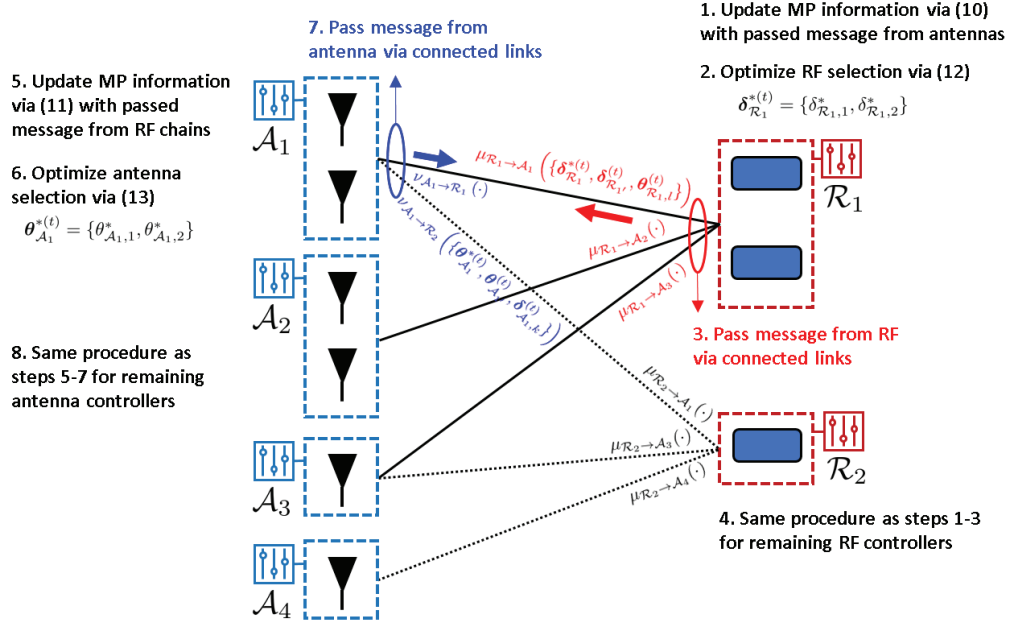


Fig. 3. The example for sequential MP of proposed MARS-S scheme considering $N_{ant}^C = 4$ antenna controllers and $N_{RF}^C = 2$ RF chain controllers.

its own solution based on the received information from the neighboring controllers. That is, only one controller conducts MP while the others wait for the completion of message transfer. Therefore, the k -th RF controller will employ MP operation of $\mu_{\mathcal{R}_k \rightarrow \mathcal{A}_l} \left(\{\delta_{\mathcal{R}_k}^{*(t)}, \delta_{\mathcal{R}_{k'}}^{(t)}, \theta_{\mathcal{R}_{k,l}}^{(t)}\} \right)$ to pass its optimal RF selection $\delta_{\mathcal{R}_k}^{*(t)}$ at the t -th iteration along with the updated information given in (9). Similarly, the l -th antenna controller will transfer the optimal antenna selection and update information using $\nu_{\mathcal{A}_l \rightarrow \mathcal{R}_k} \left(\{\theta_{\mathcal{A}_l}^{*(t)}, \theta_{\mathcal{A}_{l'}}^{(t)}, \delta_{\mathcal{A}_{l,k}}^{(t)}\} \right)$.

The concrete scheme of the proposed MARS-S as a sequential MP is described in Algorithm 2, which is also depicted in Fig. 3. All parameters will be initialized randomly along with the measured channel information. Firstly, the RF chain controller will update its decision according to the received message based on (9). Note that we consider a randomized update method to prevent a local optimum, i.e., the optimization of (11) is obtained when $x \leq \eta_r$, where x is a random variable between $[0, 1]$ and η_r is the predefined learning rate. After obtaining the temporary optimal RF selection $\delta_{\mathcal{R}_k}^{*(t)}$ constrained by (7c), the k -th RF chain controller will pass the decision and update the set of $\{\delta_{\mathcal{R}_k}^{*(t)}, \delta_{\mathcal{R}_{k'}}^{(t)}, \theta_{\mathcal{R}_{k,l}}^{(t)}\}$ to the neighboring antenna controllers. The antenna controllers can perform their operations until the completion of RF controllers. Afterwards, the antenna controllers adopt a similar process as that of RF chain controller to update, optimize, and pass message. The update of antennas is based on (10), whilst

Algorithm 2: Proposed MARS-S Scheme

```

1: Initialization:  $\mathbf{W}_{\text{BB}}, \mathbf{W}_{\text{RF}}, \mathbf{H}, \mathbf{C}, \delta, \theta, \eta_r, \eta_a, \kappa, t = 1$ 
2: Perform channel estimation  $\mathbf{H}$ 
3: Randomize beamformer of  $\mathbf{W}_{\text{BB}}, \mathbf{W}_{\text{RF}}$ 
4: Obtain LDPC-based connection based on Algorithm 1
5: BS broadcasts above information to each controller
6: repeat
7:   (RF Chain Controller)
8:   for  $\mathcal{R}_k \in \mathcal{R}^c$  do
9:     Update the  $k$ -th RF controller's information based on (9)
10:    Randomly generate a number  $x \in [0, 1]$ 
11:    if  $x \leq \eta_r$  then
12:      Obtain the temporary optimized RF chain selection  $\delta_{\mathcal{R}_k}^{*(t)}$  according to (11)
13:      Reselect RF chains if (7c) is not satisfied
14:    end if
15:    Pass the updated and optimized message to neighboring connected controllers as  $\mu_{\mathcal{R}_k \rightarrow \mathcal{A}_l} \left( \{\delta_{\mathcal{R}_k}^{*(t)}, \delta_{\mathcal{R}_{k'}}^{(t)}, \delta_{\mathcal{A}_l, k}^{(t)}\} \right)$ 
16:  end for
17:  (Antenna Controller)
18:  for  $\mathcal{A}_l \in \mathcal{A}^c$  do
19:    Update the  $l$ -th antenna controller's information according to (10)
20:    Generate a random number  $x \in [0, 1]$ 
21:    if  $x \leq \eta_a$  then
22:      Derive the temporary optimized antenna selection  $\theta_{\mathcal{A}_l}^{*(t)}$  according to (12)
23:      Reselect antennas if (8c) is not fulfilled
24:    end if
25:    Pass the updated and optimized message to neighboring connected controllers as  $\nu_{\mathcal{A}_l \rightarrow \mathcal{R}_k} \left( \{\theta_{\mathcal{A}_l}^{*(t)}, \theta_{\mathcal{A}_{l'}}^{(t)}, \delta_{\mathcal{A}_l, k}^{(t)}\} \right)$ 
26:  end for
27:  (Optimum Derivation)
28:  Optimum of RF/antenna selection is  $\{\delta^*, \theta^*\} = \{\delta^{(t)}, \theta^{(t)}\}$ 
29:  Iteration update  $t = t + 1$ 
30: until Convergence of  $|P(\delta^{(t-1)}, \theta^{(t-1)}) - P(\delta^{(t)}, \theta^{(t)})| \leq \kappa$ 

```

the optimization follows (12) constrained by (8c). Note that the optimal outcome can be acquired if the randomized value of x is smaller than the given learning rate of η_a for antenna selections. Then, the l -th antenna controller will transfer the decision and update the set of $\{\theta_{\mathcal{A}_l}^{*(t)}, \theta_{\mathcal{A}_{l'}}^{(t)}, \delta_{\mathcal{A}_l, k}^{(t)}\}$ to the connected RF controllers. The convergence occurs when the difference of power consumption between these two iterations are smaller than a given threshold, i.e., $|P(\delta^{(t-1)}, \theta^{(t-1)}) - P(\delta^{(t)}, \theta^{(t)})| \leq \kappa$.

B. MARS-P of Parallel Message Passing

We can infer from MARS-S that it potentially induces low convergence speed due to the sequential operation of MP. The adjacent controllers should wait until the completion of their connected controllers. Therefore, we conceive a parallel MP type as MARS-P so that all RF/antenna controllers can simultaneously pass their optimized determinations. The steps of proposed MARS-P scheme is similar to that

how parallel MP conveys information. The detailed algorithm of MARS-P is elaborated in Algorithm 3, which allows all controllers to simultaneously transmit message without waiting time. The example to demonstrate the process of MARS-P is illustrated in Fig. 4. However, due to simultaneous update in MARS-P, the controller potentially suffers from the local decision leading to low convergence rate. Therefore, similar to MARS-S, we also need to design a feasible learning rate parameter to strike a compelling tradeoff between convergence and local optimum.

To elaborate a little further, the proposed MARS scheme can be used in both narrowband and wideband systems. There are two ways to modify the MARS algorithms for these systems. The first method is through an **average** manner, which involves estimating the wideband channel state information using a single parameter with the dimension of the multiplied numbers of transmitters and receivers. However, this approach results in lower complexity but worse performance due to the coarse channel estimation compared to the fine-grained sub-channel optimization. The second scheme is through a **sub-channel**-based perspective, which provides better performance but is more complicated due to the coupled total power among sub-channels. This may result in a trade-off among different sub-channels, where selecting a certain sub-channel may be harmful to another. To address this issue, an alternative optimization approach can be designed by adding an additional iteration loop to iteratively search over each sub-channel until convergence. This approach allows us to apply the existing MARS algorithm directly in a wideband scenario, but it may require additional computational complexity depending on the number of sub-channels being operated. Moreover, it is worth noticed that advanced beamforming can be designed to further enhance the system performance, whereas this work can be regarded as a lower bound of joint optimization of both RF/antenna selection and beamformer design, which requires additional complex mechanism in the future.

C. Complexity Analysis

The computational complexity is demonstrated in Table II. We can know that the joint solution for the conventional full-connection HBF architecture in problem (5) requires an exponential complexity of $\mathcal{O}(2^{N_{RF}N_{ant}})$ which leads to a potential difficulty to acquire the global optimum. On the other hand, the proposed MARS scheme possess a much lower computational complexity than exhaustive search of the original problem, i.e., MARS-S as a sequential MP scheme achieves a complexity of $\mathcal{O}(2^{|\mathcal{R}^c|N_{RF,k}+|\mathcal{A}^c|N_{ant,l}})$, whereas the parallel type mechanism of MARS-P possesses a complexity of $\mathcal{O}(2^{N_{RF,k}+N_{ant,l}})$. It can be observed that MARS-S has a higher computational complexity than

TABLE II
COMPUTATIONAL COMPLEXITY

Algorithm	Complexity
Global Optimum	$\mathcal{O}(2^{N_{RF}N_{ant}})$
Proposed MARS-S	$\mathcal{O}(2^{ \mathcal{R}^c N_{RF,k} + \mathcal{A}^c N_{ant,l}})$
Proposed MARS-P	$\mathcal{O}(2^{N_{RF,k} + N_{ant,l}})$
Greedy-based Selection	$\mathcal{O}(\mathcal{R}^c N_{RF,k} + \mathcal{A}^c N_{ant,l})$
Genetic-based Selection	$\mathcal{O}(N_{crx}N_{RF}N_{ant} + N_{mu})$

TABLE III
SYSTEM PARAMETER SETTING

Parameters	Value
Carrier frequency f_c	28 GHz
Distance between transmitter and receiver d	100 meters
Number of data streams N_S	4
Transmit power P_T	46 dBm
Noise power N_0	-85 dBm
Power consumption of an RF chain P_{RF}	40 mWatt
Power consumption of baseband processing P_{BB}	800 mWatt
Power consumption of ADC P_{ADC}	100 mWatt
Power consumption of a phase shifter P_{PS}	10 mWatt
Power consumption of a LNA P_{LNA}	10 mWatt
Maximum output power for antenna elements P_o	25 dBm
Maximum allowable system power P_{max}	42 dBm
Threshold of RF/antenna selection η_r, η_a	0.7

MARS-P due to the sequential MP mechanism. The RF/antenna controllers will update their latest information and then determine the corresponding selection results which leads to no existence of missed message. Comparing to the existing works, the greedy-based selection [39] only cares for single antenna policy with others fixed, which has a complexity order of $\mathcal{O}(|\mathcal{R}^c|N_{RF,k} + |\mathcal{A}^c|N_{ant,l})$. Moreover, the genetic-based selection method [40] adopting genetic generation, elite selection, crossover and mutation possesses a complexity order of $\mathcal{O}(N_{crx}N_{RF}N_{ant} + N_{mu})$, where N_{crx} and N_{mu} denote the number of crossover and mutation times, respectively. Note that since both papers [39], [40] only consider antenna selection, we therefore adjust the genetic and greedy selection to also consider the RF selection problem for fair comparison. Owing to simultaneous passed information in MARS-P, there may have either missed or out-of-date information which potentially provokes a local optimum. However, compared to the full-connection of HBF scheme in the original problem, the proposed MARS scheme reach the lowest computational complexity while sustaining the nearly-optimal solution acquirement.

V. PERFORMANCE EVALUATION

The performance of proposed MARS scheme is evaluated via simulations. We consider a downlink transmission with a single transmitter and a hybrid beamformed-MIMO receiver. The distance between transmitter and receiver is set as $d = 100$ meters, and the operating carrier frequency is $f_c = 28$ GHz. Transmit power is set as maximum value of 46 dBm. The values of receiver power consumption utilized in our simulation are given by $P_{RF} = 40$ mWatt, $P_{BB} = 800$ mWatt, $P_{ADC} = 100$ mWatt, and $P_{PS} = P_{LNA} = 10$ mWatt [41]–[44]. The maximum output power for insertion loss of antenna elements if $P_o = 25$ dBm, and allowable system power is $P_{max} = 42$ dBm. The parameter $\rho = 10^{-PL/10}$ referring distance-based pathloss where $PL = 32.4 + 20 \log_{10}(f_c) + 30 \log_{10}(d)$ [45]. The learning rate threshold of RF/antenna selection is given as $\eta_r = \eta_a = 0.7$. For simulation simplicity, we consider equivalent number of elements in each RF/antenna group, i.e., $N_{RF,k} = N_{RF}^G$ and $N_{ant,l} = N_{ant}^G, \forall k, l$. The related outcome is characterized by power consumption (W) and corresponding EE (bits/J/Hz)³, i.e., $EE = R(\Delta, \Theta)/P(\delta, \theta)$. The pertinent system parameters are listed in Table III.

A. Convergence and Learning Rate

As illustrated in Fig. 5, convergence of proposed MARS scheme is validated through simulations. We can infer from both figures that proposed MARS-S achieves lower power consumption and higher EE than that of MARS-P. This is because sequential passing can let up-to-date decisions be completely conveyed to other nodes in order, whereas the parallel scheme potentially confuses RF/antenna controllers with multiple simultaneous received information. This will result in worse information update and corresponding low-performance policy. Moreover, owing to attainable better policy from MARS-S, it requires more iterations to reach convergence. That is, MARS-S needs around 22 iterations for power consumption of around 11.28 W and EE of 0.84 bits/J/Hz, whilst MARS-P converges with higher power consumed and lower EE at the 13-th round, which strikes a compelling tradeoff between convergence speed and high performance.

In Fig. 6, we evaluate the performance of power consumption and EE of proposed MARS scheme under different learning rates $\eta_a \in \{0.1, 0.3, 0.5, 0.7, 0.9\}$ for antenna selection and $\eta_r \in \{0.1, 0.5, 0.9\}$ for RF chain one. Note that we consider the same number of RF/antenna elements per group as $N^G = N_{RF}^G = N_{ant}^G \in \{1, 4\}$. We can observe from Figs. 6(a) and 6(b) that higher learning rates result in

³'W' stands for the unit of "Watt", whilst 'J' is abbreviation of "Joule" which is multiplication of time in seconds (s) and power in Watt.

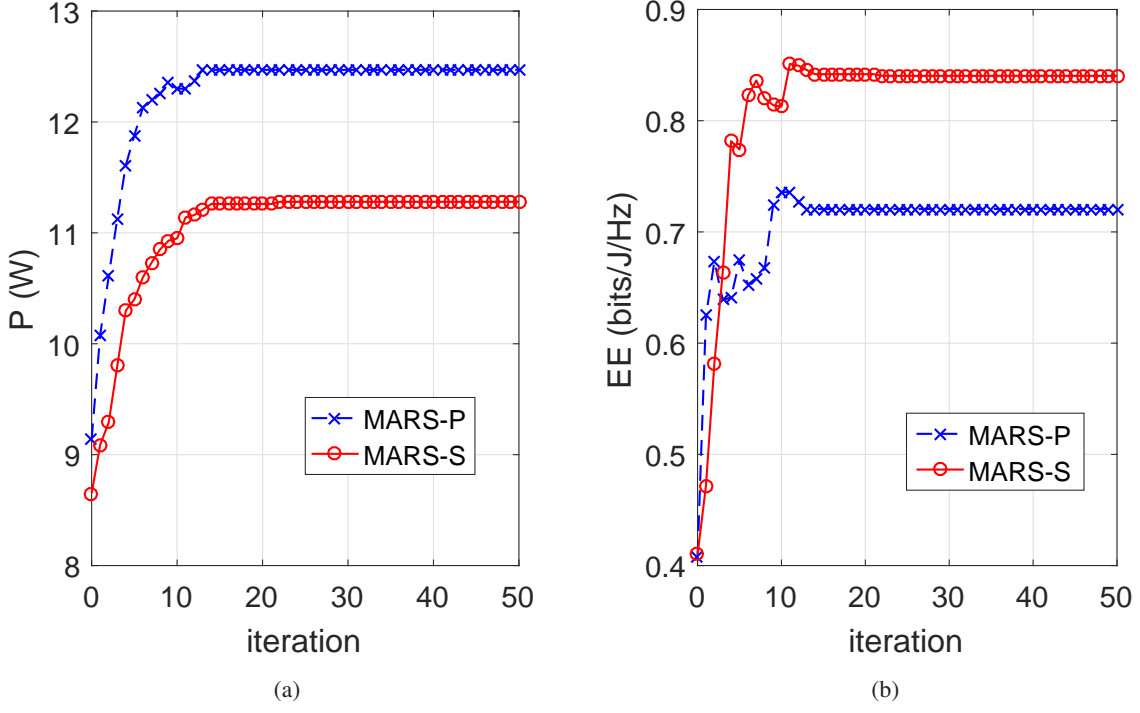


Fig. 5. Convergence of proposed MARS-S and MARS-P sub-schemes in terms of (a) power consumption and (b) EE.

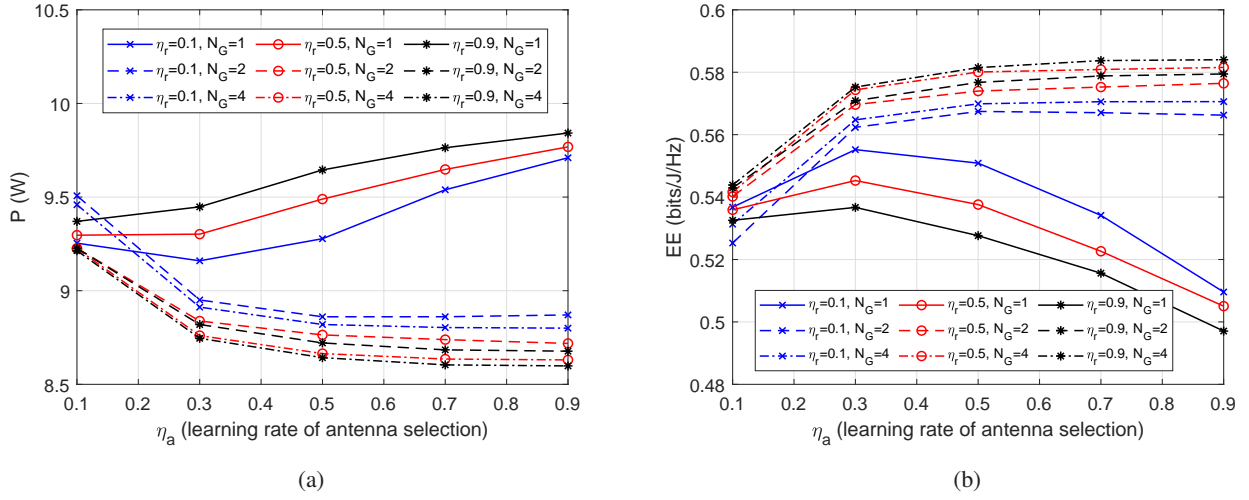


Fig. 6. Performance of proposed MARS scheme considering different learning rates of antenna selection $\eta_a \in \{0.1, 0.3, 0.5, 0.7, 0.9\}$ and RF selection $\eta_r \in \{0.1, 0.5, 0.9\}$ with elements in each RF/antenna group as $N_G = N_{RF}^G = N_{ant}^F \in \{1, 2, 4\}$ with respect to (a) power consumption and (b) EE.

lower power consumption and higher EE under more nodes managed by RF/antenna controllers, i.e., $N_G \in \{2, 4\}$. This is because that quicker policy update can prevent out-of-date information conveying to

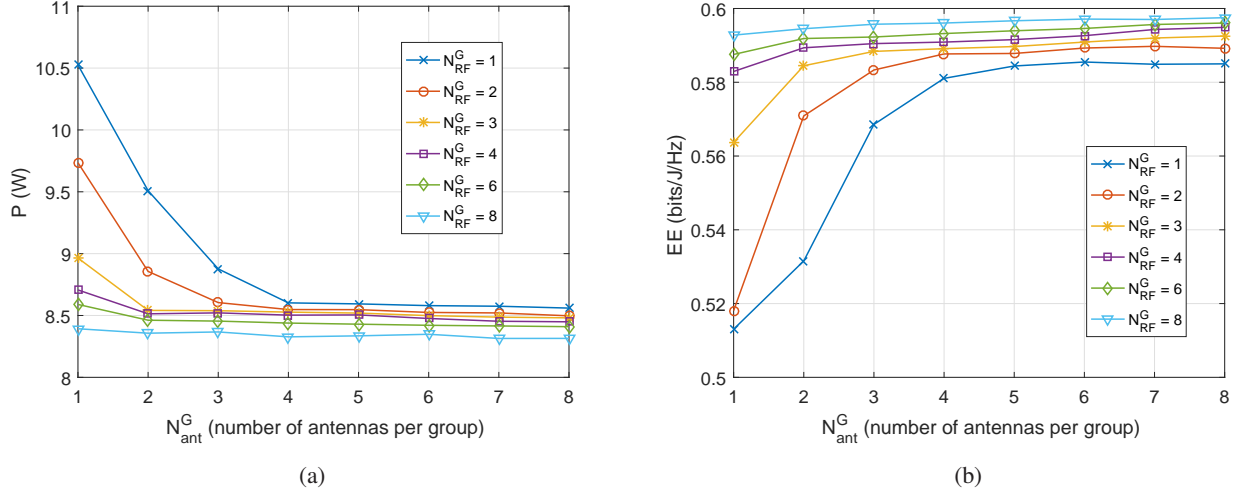


Fig. 7. Performance of MARS with various numbers of clustered RF/antennas in respective groups $N_{RF}^G \in \{1, 2, 3, 4, 6, 8\}$ and $N_{ant}^G \in \{1, 2, 3, 4, 5, 6, 7, 8\}$ with respect to (a) power consumption and (b) EE.

other controllers under a more centralized architecture, which requires shorter hops to convey decision policy. However, under a more distributive architecture with fewer numbers of nodes per group of $N_G = 1$, faster rate of $\eta_a = 0.9$ consumes more power up to averaged 9.75 W since the latest optimal message cannot be transferred to faraway nodes before next update. The best policy is potentially mantled by newly passed message from neighboring controllers. Moreover, they perform concave EE curves for $N_G = 1$ due to moderate update speed, where the optimum is attained when $\eta_a = 0.3$ as shown in Fig. 6(b).

B. Different RF/Antenna Configurations

As performed in Fig. 7, we evaluate the effects of different numbers of RF/antenna elements in each clustered group. We can observe from Fig. 7(a) that a more centralized architecture with more number of antennas per group achieves lower power consumption when $N_{RF}^G \in \{1, 2, 3\}$. The first reason for this phenomenon is that the controller is capable of obtaining a nearer-optimal solution with higher degree of freedom of selecting on-off policy. While, the other reason is due to shorter paths conveying the determined message from one group to the others, which reveals similar effects as illustrated in Fig. 6. Furthermore, it performs flatter curves for $N_{RF}^G \in \{4, 6, 8\}$ since selection of RF chains with considerably higher power consumption becomes more dominant than that of antenna selection. This also implies that fewer RF controllers is potentially able to provide a better policy with lower power consumption and accordingly higher EE performance.

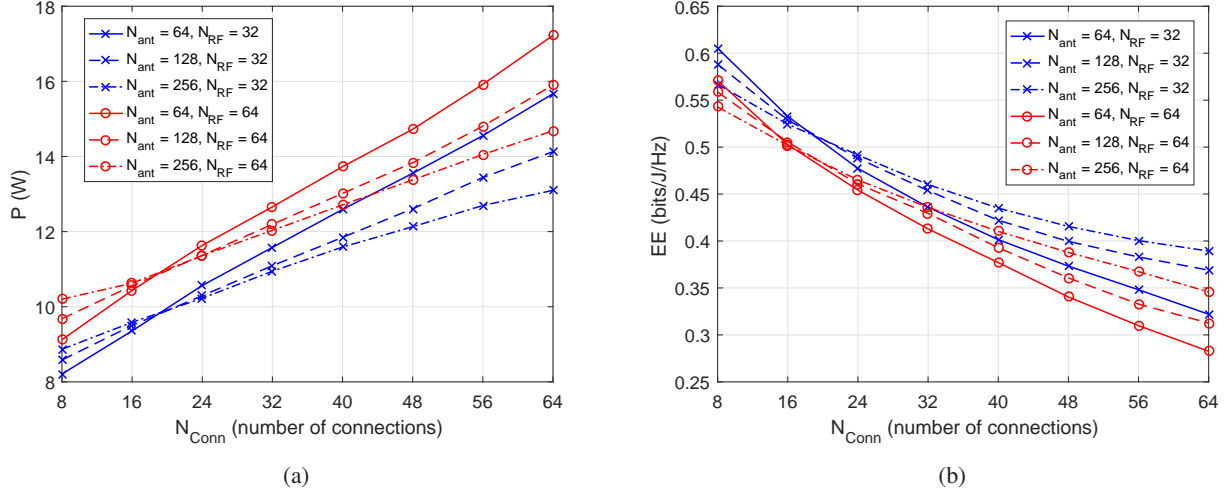


Fig. 8. Effect of different numbers of connections $N_{conn} \in \{8, 16, 24, 32, 40, 48, 56, 64\}$ with $N_{RF} \in \{32, 64\}$ RF chains and $N_{ant} \in \{64, 128, 256\}$ antennas in terms of (a) power consumption and (b) EE.

In Fig. 8, we have studied the impact of proposed MARS under different numbers of connections among RF/antenna controllers and nodes from $N_{Conn} = 8$ to 64 with $N_{RF} \in \{32, 64\}$ RF chains and $N_{ant} \in \{64, 128, 256\}$ antennas. Recall that N_{Conn} is the number of antennas associated to a single RF chain, which implies the tendency to become a fully-connected beamformer. When $N_{Conn} = 64$, it has the highest power consumption and lowest EE due to simultaneous message passed from nodes in different groups, which leads to more uncertain and complex decision making. For example, an RF controller will update distinct various message delivered from massive antenna groups connected to it, which may result in a more inappropriate update and corresponding local solution. Moreover, more antennas result in less power consumption due to higher degree of freedom of selection, e.g., power reduces from 17 W to 14.6 W considering $N_{ant} = 64$ increased to $N_{ant} = 256$ antennas for $N_{RF} = 64$ RF chains and $N_{Conn} = 64$. However, RF selection performs reverse trend because it possesses dominant operating power and lower selection freedom than antennas, which consumes around 1 W higher power when $N_{RF} = 64$ than that of $N_{RF} = 32$ for $N_{ant} = 64$ antennas and $N_{Conn} = 64$. To elaborate a little further, we can observe that another phenomenon takes place when we have the fewest connections of $N_{Conn} \in \{8, 16\}$. Higher number of antennas under fewer links will potentially cause some optimal messages missed in current iteration but being confused by other irrelevant information, deteriorating system performance.

As depicted in Fig. 9, performance of proposed MARS is evaluated considering different insertion

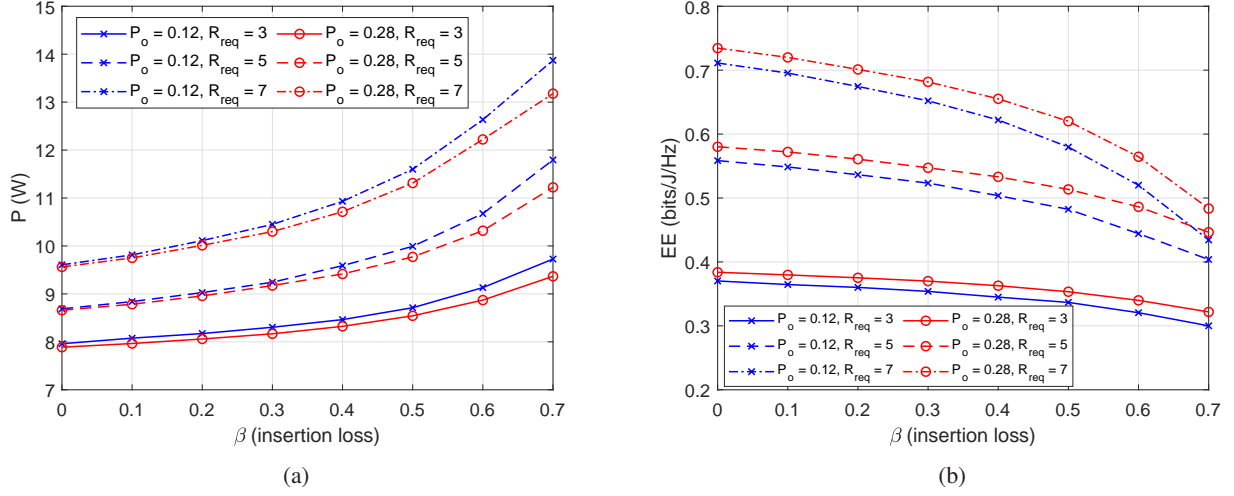


Fig. 9. Performance of proposed MARS scheme under different values of insertion losses $\beta \in \{0, 0.1, 0.2, 0.3, 0.4, 0.5, 0.6, 0.7\}$, maximum antenna output power $P_o \in \{0.12, 0.28\}$ W, and QoS $R_{req} \in \{3, 5, 7\}$ bits/s/Hz in terms of (a) power consumption and (b) EE.

losses and maximum antenna output power as well as QoS constraints. We can observe from both the received signal in (1) and throughput in (3) that both of them are monotonically decreasing and concave with respect to β . This provokes more consumed power compensated for the increment of insertion losses, which performs monotonically increasing convex shapes as seen in Fig. 9(a). Moreover, relaxed antenna output power restriction, i.e., $P_o = 0.28$ W requires lower power consumption due to attainable higher degree of freedom of RF/antenna selections. Similarly, without insertion loss of $\beta = 0$, little difference of power consumption can be observed due to relaxed constraint in (5g). Accordingly, most of power can be utilized mainly for QoS satisfaction not for compensation of insertion losses. With the increased demand of rate, more power is intuitively required with higher QoS requirement, e.g., we need around 2 W more power in most cases when QoS escalates from 3 to 7 bits/s/Hz. Moreover, as illustrated in Fig. 9(b), decreasing EE curves would intersect with β larger than 0.7 and QoS of $\{5, 7\}$ bits/s/Hz due to the fact it requires considerably higher power for QoS $R_{req} = 7$ bits/s/Hz in order to simultaneously compensate compelling hardware losses as well as QoS satisfaction.

C. Benchmarking

In Fig. 10, we have conducted performance comparison under different architectures, i.e., full-connection [22]–[24], fixed partial-connection [18], [46], [47], dynamic partial-connection designed in [21] and proposed LDPC-based architecture considering different numbers of RF/antenna elements per

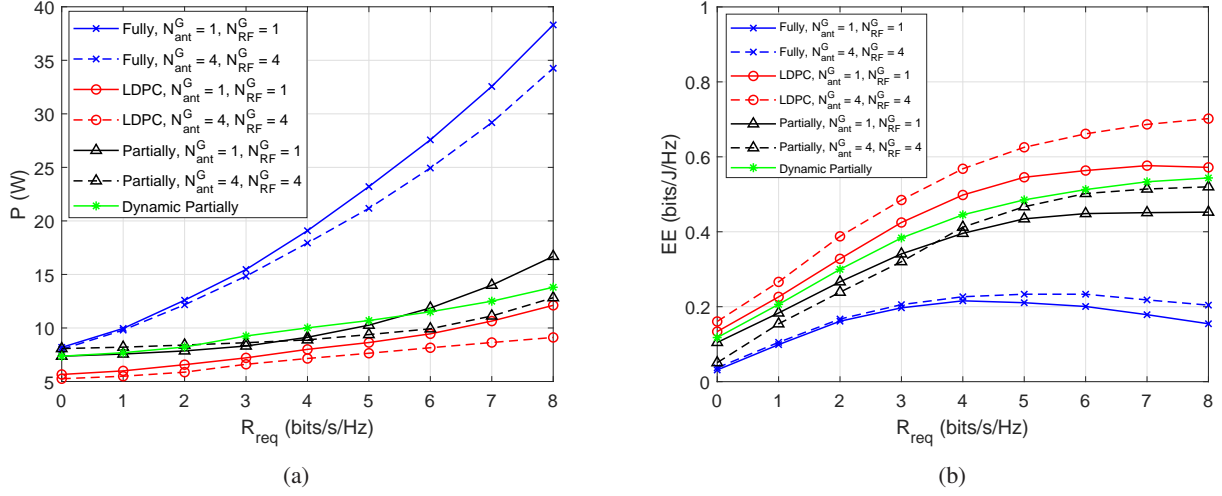


Fig. 10. Performance comparison under different architectures of fully-, partially-, dynamic partially- and LDPC-based connections with RF/antenna elements per group $N_{ant}^G = N_{RF}^G \in \{1, 4\}$ and QoS requirements $R_{req} \in \{0, 1, 2, 3, 4, 5, 6, 7, 8\}$ bits/s/Hz in terms of (a) power consumption and (b) EE. Note that dynamic partially-connection is adjustable in each sub-array sizes, so parameters of $N_{ant}^G = N_{RF}^G$ are not set.

group and QoS requirements. Note that we have also compared two different types of partial-connections. Dynamic partial connection in [21] is performed by exhaustively obtaining the optimal sub-array patterns, i.e., each sub-array has different sizes of elements but is fully-connected in its group the same as the fixed case. This potentially provides a higher degree of freedom to construct high-EE partial connection, which accordingly achieves a higher EE with similar power consumption to the fixed partially-connected architecture. Moreover, as explained previously, it requires more power to satisfy higher QoS demands, especially under fully-connected architecture with excessive power consumption up to about 35 W. As for partial connection, it results in around 3 to 5 W more power utilization compared to the proposed LDPC-based architecture since the controllers with partial connection cannot acquire certain message passed from some nodes leading to worse solutions. Furthermore, higher difference of power is induced by higher QoS requirements by comparing distributed control architecture of $N_{ant}^G = N_{RF}^G = 1$ and a centralized one with $N_{ant}^G = N_{RF}^G = 4$. This is due to the reason that some information in distributed architecture has to be conveyed from faraway nodes with massive hops generating out-of-date policy to fulfill high QoS, as also seen from Fig. 7. To elaborate a little further, we can observe opposite trends for partially-connected method. Under lower QoS $R_{req} \leq 3$ bits/s/Hz, controllers under a more distributed manner, i.e., $N_{ant}^G = N_{RF}^G = 1$, will tend to greedily optimize itself due to unknown or non-updated message passed from others. By contrast, a more centralized one with $N_{ant}^G = N_{RF}^G = 4$

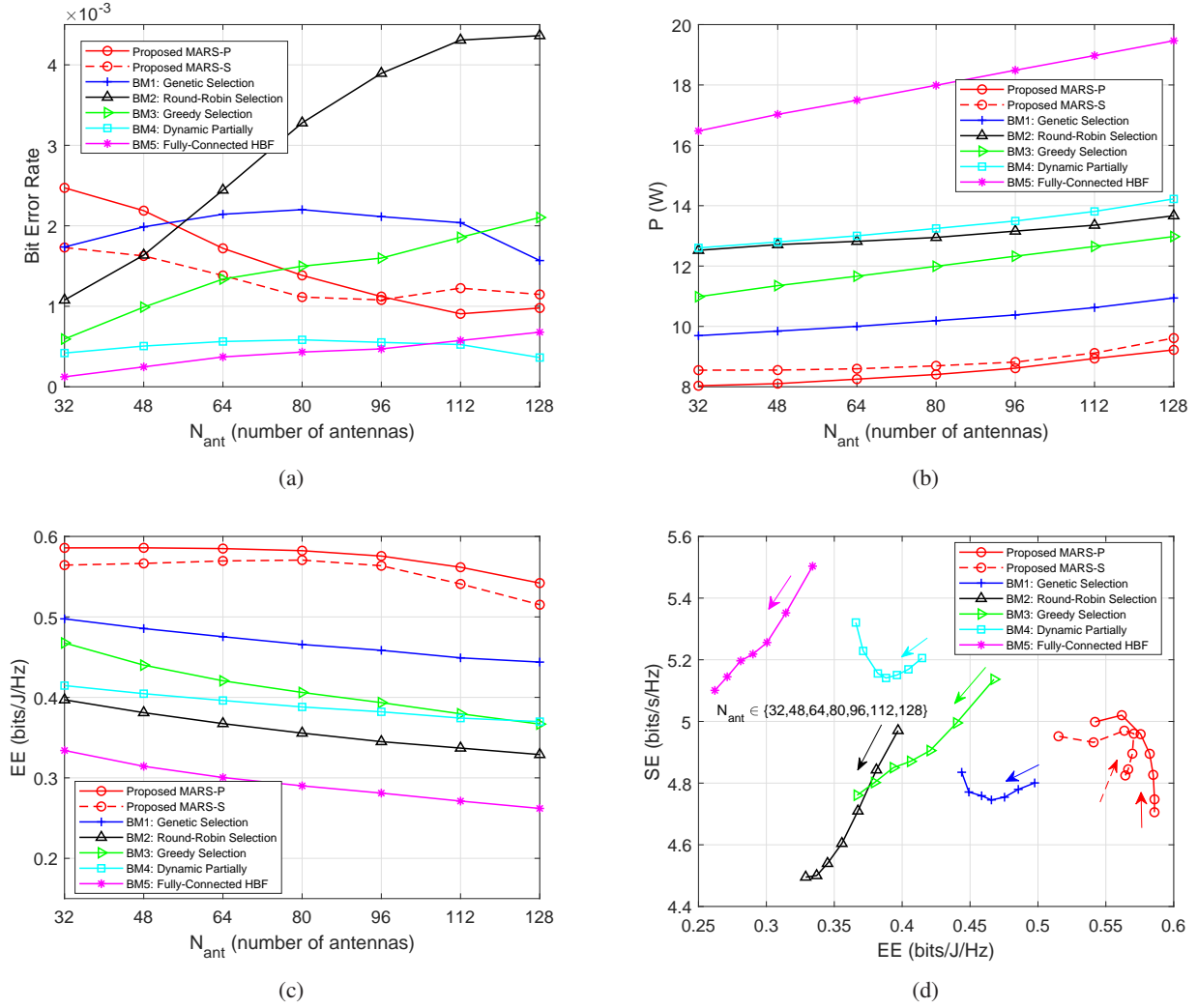


Fig. 11. Performance comparison of proposed MARS scheme and benchmarks of genetic-, greedy- and round-robin-based selection with numbers of receiving antennas $N_{ant} \in \{32, 48, 64, 80, 96, 112, 128\}$ in terms of (a) bit error rate, (b) power consumption, (c) EE, and (d) spectrum-energy efficiency. Note that the direction of arrows indicates the increment of N_{ant} .

is able to provide more appropriate policy with adequate QoS-aware information achieving comparably lower power and accordingly higher EE. To conclude, the proposed LDPC-based architecture under MARS scheme can respectively conserve around 25 W and 5 W and improve about 250% and 40% of EE compared to fully-/partially-connected structures.

In Fig. 11, we compare the comprehensive performances of bit error rate (BER), power consumption, EE, and spectrum-energy efficiency for the proposed MARS scheme of MARS-P and MARS-S with five benchmarks (BMs) as elaborated as follows. Note that we consider equivalent QoS constraint of $R_{req} = 3$ bits/s/Hz, insertion loss $\beta = 0.3$, $N_{RF} = 32$, $N_{RF}^G = N_{ant}^G = 4$ for a fair comparison.

- **BM1 Genetic-based Selection** [40]: The selection solution is initially provided with a given number of genetic population. The candidate solution is obtained by adopting discrete genetic algorithm with cross-over, mutation, elite selection and offspring gene generation. Note that all RF chains are selected to operate, i.e., $\delta_n = 1 \forall n \in \mathcal{R}$. This case is conducted based on the designed LDPC-based connection.
- **BM2 Round-Robin Selection**: The candidate solution of RF/antenna selection is randomly initialized and evaluated via round robin manner. We transfer the mechanism in [48] from MIMO user scheduling to RF/antenna selection. Note that either policy under fully-off antennas or RF chains is excluded here due to zero rate performance. This case is conducted based on the designed LDPC-based connection.
- **BM3 Greedy-based Selection** [39]: It optimizes the policy of single antenna with the other solutions fixed, which can be regarded as a distributed manner with $N_{ant}^G = 1$ in this work. We firstly randomly conduct antenna selection of either turning on or off for all nodes. Afterwards, we iteratively select the one in a selfish manner that leads to the lowest power consumption until the completion of the final node. Note that all RF chains are selected to be under operation, i.e., $\delta_n = 1 \forall n \in \mathcal{R}$. This case is conducted based on the designed LDPC-based connection.
- **BM4 Dynamical Partially** [21]: This connection is performed by exhaustively obtaining the optimal sub-array patterns, i.e., each sub-array has different sizes of elements but is fully-connected in its subgroup the same as the fixed case, which provides a higher degree of freedom than that of partial-connection with equal sub-array size. All RF chains and antennas in each sub-array are selected to be operated.
- **BM5 Fully-Connected HBF** [49]: Conventional HBF architecture is conducted under a full-connection with whole RF chains and antennas selected to be operated.

In Fig. 11(a), we can observe that BMs 4 and 5 have the lowest BER due to more connected links in HBF, i.e., more information with higher degree of freedom can be attained to achieve higher rate. BMs 1 and 3 possess medium performance of BER under LDPC architecture. With similar performance, the proposed MARS scheme has lower BER with more antennas owing to more passed information. Round-robin potentially switches off beneficial nodes, leading to the worst BER. To elaborate a little further, BER will reflect the negative correlation in performances of spectrum efficiency (SE) as shown in Fig. 11(d), i.e., lower BER will achieve higher SE. We can infer from Fig. 11(b) that more power is required to operate the increased number of deployed antennas. Considering LDPC architecture, however, BM2

requires the highest power due to random selection without any information utilized. As for BM3, a selfish-style method is employed to optimize its own antenna selection without using message from other controller groups. However, as a compromised mechanism in BM1, genetic-based selection takes into account selection policy from other groups, which preserves power of 2.8 W and 2 W compared to round-robin and greedy selection under $N_{ant} = 128$, respectively. By contrast, BM4 regarded as the optimal solution in partial-connection requires a bit more power than the baseline solution in LDPC architecture due to comparably fewer links required to achieve satisfying services. Moreover, BM5 with full-connected consumes the most power resources, which is around twice more than that of proposed MARS schemes.

Although MARS-P possesses faster policy update speed, it potentially leads to missed information due to parallel transfer of message passing, which has slightly higher power of about 0.5 W compared to sequential manner in MARS-S. Benefited by both LDPC connection as well as message passing based design, the proposed MARS can exactly convey appropriate information to all the other controller groups to attain a better RF/antenna selection policy. In this context, observed from Figs. 11(b) and 11(c) considering $N_{ant} = 128$, the proposed MARS scheme outperforms all the benchmarks, which is able to preserve power of about 1.8, 3.8, 4.6, 5 and 10.2 W and to improve around 22%, 46%, 50%, 68% and 107% of EE compared to BMs 1 to 5, respectively. Furthermore, as can be seen in Fig. 11(d), it also strikes a tradeoff between SE and EE metrics. MARS accomplishes the highest EE at the expense of moderate throughput, whilst full-connection alternatively has the highest rate by consuming the most power leading to the lowest EE. Also, it is noticed that BMs 1 and 4 perform the asymptotic shape of curve due to the optimal solution is potentially obtained from genetic selection with lower searching space.

VI. CONCLUSION

In this paper, we have conceived an LDPC-based HBF structure and MARS scheme to jointly consider RF chain and antenna selection for minimization of operating power consumption, which is guaranteed by QoS and available power utilization. MARS can be employed under sequential (MARS-S) and parallel (MARS-P) message passing under either distributed or centralized architecture. The performance reveals that MARS-P has faster convergence than MARS-S due to parallel information delivery. However, MARS-S achieves lower power consumption and higher EE due to non-overlapped decisions from fewer neighboring nodes. Additionally, missed message or out-of-date policy is resolved by selecting

appropriate learning rates for RF chains and antenna selections. Due to dominant RF chains, performance is more significantly influenced by RF chains than antennas under different numbers of controllers, connections, and hardware impairment effects. Moreover, the proposed LDPC-based structure with MARS achieves the lowest power and highest EE since it possesses considerably fewer links than full-connection but with more information exchanged than partially-connected architecture. Additionally, benefited by better message and policy passed from other RF/antenna nodes, MARS outperforms the existing algorithms of round-robin, greedy-based, genetic-based selection methods as well as dynamic adjustment of partial-/full-connection in open literature.

REFERENCES

- [1] W. Saad, M. Bennis, and M. Chen, "A vision of 6G wireless systems: Applications, trends, technologies, and open research problems," *IEEE Network*, vol. 34, no. 3, pp. 134–142, 2020.
- [2] L.-H. Shen, K.-T. Feng, and L. Hanzo, "Five facets of 6G: Research challenges and opportunities," *ACM Computing Surveys*, vol. 55, no. 11, pp. 1–39, 2023.
- [3] H. Zhang, S. Huang, C. Jiang, K. Long, V. C. M. Leung, and H. V. Poor, "Energy efficient user association and power allocation in millimeter-wave-based ultra dense networks with energy harvesting base stations," *IEEE Journal on Selected Areas in Communications*, vol. 35, no. 9, pp. 1936–1947, 2017.
- [4] T. Huang, W. Yang, J. Wu, J. Ma, X. Zhang, and D. Zhang, "A survey on green 6G network: Architecture and technologies," *IEEE Access*, vol. 7, pp. 175 758–175 768, 2019.
- [5] S. Yang and L. Hanzo, "Fifty years of MIMO detection: The road to large-scale MIMO," *IEEE Communications Surveys Tutorials*, vol. 17, no. 4, pp. 1941–1988, 2015.
- [6] Q.-U.-A. Nadeem, A. Kammoun, and M.-S. Alouini, "Elevation beamforming with full dimension MIMO architectures in 5G systems: A tutorial," *IEEE Communications Surveys Tutorials*, vol. 21, no. 4, pp. 3238–3273, 2019.
- [7] S. Kutty and D. Sen, "Beamforming for millimeter wave communications: An inclusive survey," *IEEE Communications Surveys Tutorials*, vol. 18, no. 2, pp. 949–973, 2016.
- [8] S. Han, C.-I. I. Z. Xu, and C. Rowell, "Large-scale antenna systems with hybrid analog and digital beamforming for millimeter wave 5G," *IEEE Communications Magazine*, vol. 53, no. 1, pp. 186–194, 2015.
- [9] S. S. Ioushua and Y. C. Eldar, "A family of hybrid analog–digital beamforming methods for massive MIMO systems," *IEEE Transactions on Signal Processing*, vol. 67, no. 12, pp. 3243–3257, 2019.
- [10] I. Ahmed, H. Khammari, A. Shahid, A. Musa, K. S. Kim, E. De Poorter, and I. Moerman, "A survey on hybrid beamforming techniques in 5G: Architecture and system model perspectives," *IEEE Communications Surveys Tutorials*, vol. 20, no. 4, pp. 3060–3097, 2018.
- [11] L.-H. Shen and K.-T. Feng, "Mobility-aware subband and beam resource allocation schemes for millimeter wave wireless networks," *IEEE Transactions on Vehicular Technology*, vol. 69, no. 10, pp. 11 893–11 908, 2020.
- [12] Y. Cai, Y. Xu, Q. Shi, B. Champagne, and L. Hanzo, "Robust joint hybrid transceiver design for millimeter wave full-duplex MIMO relay systems," *IEEE Transactions on Wireless Communications*, vol. 18, no. 2, pp. 1199–1215, 2019.
- [13] L.-H. Shen, Y.-C. Chen, and K.-T. Feng, "Design and analysis of multi-user association and beam training schemes for millimeter wave based WLANs," *IEEE Transactions on Vehicular Technology*, vol. 69, no. 7, pp. 7458–7472, 2020.

- [14] L.-H. Shen, K.-T. Feng, and L. Hanzo, "Coordinated multiple access point multiuser beamforming training protocol for millimeter wave WLANs," *IEEE Transactions on Vehicular Technology*, vol. 69, no. 11, pp. 13 875–13 889, 2020.
- [15] L.-H. Shen, T.-W. Chang, K.-T. Feng, and P.-T. Huang, "Design and implementation for deep learning based adjustable beamforming training for millimeter wave communication systems," *IEEE Transactions on Vehicular Technology*, vol. 70, no. 3, pp. 2413–2427, 2021.
- [16] H. Li, M. Li, Q. Liu, and A. L. Swindlehurst, "Dynamic hybrid beamforming with low-resolution PSs for wideband mmwave MIMO-OFDM systems," *IEEE Journal on Selected Areas in Communications*, vol. 38, no. 9, pp. 2168–2181, 2020.
- [17] Y. Zhang, J. Du, Y. Chen, M. Han, and X. Li, "Optimal hybrid beamforming design for millimeter-wave massive multi-user MIMO relay systems," *IEEE Access*, vol. 7, pp. 157 212–157 225, 2019.
- [18] Y. Zhang, J. Du, Y. Chen, X. Li, K. M. Rabie, and R. Khkrel, "Dual-iterative hybrid beamforming design for millimeter-wave massive multi-user MIMO systems with sub-connected structure," *IEEE Transactions on Vehicular Technology*, vol. 69, no. 11, pp. 13 482–13 496, 2020.
- [19] A. Morsali, A. Haghighat, and B. Champagne, "Generalized framework for hybrid analog/digital signal processing in massive and ultra-massive-MIMO systems," *IEEE Access*, vol. 8, pp. 100 262–100 279, 2020.
- [20] D. Zhang, Y. Wang, X. Li, and W. Xiang, "Hybridly connected structure for hybrid beamforming in mmwave massive MIMO systems," *IEEE Transactions on Communications*, vol. 66, no. 2, pp. 662–674, 2018.
- [21] Y. Chen, D. Chen, T. Jiang, and L. Hanzo, "Millimeter-wave massive MIMO systems relying on generalized sub-array-connected hybrid precoding," *IEEE Transactions on Vehicular Technology*, vol. 68, no. 9, pp. 8940–8950, 2019.
- [22] N. N. Moghadam, G. Fodor, M. Bengtsson, and D. J. Love, "On the energy efficiency of MIMO hybrid beamforming for millimeter-wave systems with nonlinear power amplifiers," *IEEE Transactions on Wireless Communications*, vol. 17, no. 11, pp. 7208–7221, 2018.
- [23] M. Sefunç, A. Zappone, and E. A. Jorswieck, "Energy efficiency of mmwave MIMO systems with spatial modulation and hybrid beamforming," *IEEE Transactions on Green Communications and Networking*, vol. 4, no. 1, pp. 95–108, 2020.
- [24] L. Zhao, M. Li, C. Liu, S. V. Hanly, I. B. Collings, and P. A. Whiting, "Energy efficient hybrid beamforming for multi-user millimeter wave communication with low-resolution A/D at transceivers," *IEEE Journal on Selected Areas in Communications*, vol. 38, no. 9, pp. 2142–2155, 2020.
- [25] A. Kaushik, E. Vlachos, C. Tsinos, J. Thompson, and S. Chatzinotas, "Joint bit allocation and hybrid beamforming optimization for energy efficient millimeter wave MIMO systems," *IEEE Transactions on Green Communications and Networking*, vol. 5, no. 1, pp. 119–132, 2021.
- [26] S. Payami, M. Ghoraiishi, and M. Dianati, "Hybrid beamforming for large antenna arrays with phase shifter selection," *IEEE Transactions on Wireless Communications*, vol. 15, no. 11, pp. 7258–7271, 2016.
- [27] A. Kaushik, J. Thompson, E. Vlachos, C. Tsinos, and S. Chatzinotas, "Dynamic RF chain selection for energy efficient and low complexity hybrid beamforming in millimeter wave MIMO systems," *IEEE Transactions on Green Communications and Networking*, vol. 3, no. 4, pp. 886–900, 2019.
- [28] E. Vlachos and J. Thompson, "Energy-efficiency maximization of hybrid massive MIMO precoding with random-resolution DACs via RF selection," *IEEE Transactions on Wireless Communications*, vol. 20, no. 2, pp. 1093–1104, 2021.
- [29] F. Kschischang, B. Frey, and H.-A. Loeliger, "Factor graphs and the sum-product algorithm," *IEEE Transactions on Information Theory*, vol. 47, no. 2, pp. 498–519, 2001.
- [30] J. Zeng, J. Lin, and Z. Wang, "Low complexity message passing detection algorithm for large-scale MIMO systems," *IEEE Wireless Communications Letters*, vol. 7, no. 5, pp. 708–711, 2018.

- [31] Z. Sui, S. Yan, H. Zhang, L.-L. Yang, and L. Hanzo, "Approximate message passing algorithms for low complexity OFDM-IM detection," *IEEE Transactions on Vehicular Technology*, vol. 70, no. 9, pp. 9607–9612, 2021.
- [32] N. J. Myers, J. Kaleva, A. Tölli, and R. W. Heath, "Message passing-based link configuration in short range millimeter wave systems," *IEEE Transactions on Communications*, vol. 68, no. 6, pp. 3465–3479, 2020.
- [33] Y. Jeong, C. Lee, and Y. H. Kim, "Power minimizing beamforming and power allocation for MISO-NOMA systems," *IEEE Transactions on Vehicular Technology*, vol. 68, no. 6, pp. 6187–6191, 2019.
- [34] N.-I. Kim and D.-H. Cho, "Scheduling and layer selection based performance improvement of uplink SCMA system with receive beamforming," *IEEE Transactions on Vehicular Technology*, vol. 68, no. 7, pp. 7209–7213, 2019.
- [35] Y. Yu, M. Pischella, and D. Le Ruyet, "Distributed antenna selection with message passing algorithm for MIMO D2D communications," in *Proc. IEEE International Symposium on Wireless Communication Systems (ISWCS)*, 2017, pp. 454–458.
- [36] R. Gallager, "Low-density parity-check codes," *IRE Transactions on Information Theory*, vol. 8, no. 1, pp. 21–28, 1962.
- [37] T. Richardson, M. Shokrollahi, and R. Urbanke, "Design of capacity-approaching irregular low-density parity-check codes," *IEEE Transactions on Information Theory*, vol. 47, no. 2, pp. 619–637, 2001.
- [38] O. Hiari and R. Mesleh, "Impact of RF-switch insertion loss on the performance of space modulation techniques," *IEEE Communications Letters*, vol. 22, no. 5, pp. 958–961, 2018.
- [39] M. O. K. Mendonça, P. S. R. Diniz, T. N. Ferreira, and L. Lovisolo, "Antenna selection in massive MIMO based on greedy algorithms," *IEEE Transactions on Wireless Communications*, vol. 19, no. 3, pp. 1868–1881, 2020.
- [40] J. C. Marinello, T. Abrão, A. Amiri, E. de Carvalho, and P. Popovski, "Antenna selection for improving energy efficiency in XL-MIMO systems," *IEEE Transactions on Vehicular Technology*, vol. 69, no. 11, pp. 13 305–13 318, 2020.
- [41] R. Méndez-Rial, C. Rusu, N. González-Prelcic, A. Alkhateeb, and R. W. Heath, "Hybrid MIMO architectures for millimeter wave communications: Phase shifters or switches?" *IEEE Access*, vol. 4, pp. 247–267, 2016.
- [42] H. Krishna, R. Rajakumar, and S. Chakrabarti, "Quantifying the improvement in energy savings for LTE enodeb baseband subsystem with technology scaling and multi-core architectures," in *Proc. National Conference on Communications (NCC)*, 2012, pp. 1–5.
- [43] M. Kadam, S. Aniruddhan, and A. Kumar, "An unconditionally stable 28 ghz 18 db gain LNA employing current-reuse," in *Proc. IEEE International Symposium on Circuits and Systems (ISCAS)*, 2020, pp. 1–4.
- [44] P. Skrimponis, S. Dutta, M. Mezzavilla, S. Rangan, S. H. Mirfarshbafan, C. Studer, J. Buckwalter, and M. Rodwell, "Power consumption analysis for mobile mmwave and sub-THz receivers," in *Proc. IEEE 6G Wireless Summit (6G SUMMIT)*, 2020, pp. 1–5.
- [45] 3GPP, "Study on channel model for frequencies from 0.5 to 100 GHz," no. TR 38.901 version 16.1.0 Release 16, Nov. 2020.
- [46] X. Song, T. Kühne, and G. Caire, "Fully-/partially-connected hybrid beamforming architectures for mmwave MU-MIMO," *IEEE Transactions on Wireless Communications*, vol. 19, no. 3, pp. 1754–1769, 2020.
- [47] N. T. Nguyen and K. Lee, "Unequally sub-connected architecture for hybrid beamforming in massive MIMO systems," *IEEE Transactions on Wireless Communications*, vol. 19, no. 2, pp. 1127–1140, 2020.
- [48] H. A. Ammar, R. Adve, S. Shahbazpanahi, G. Boudreau, and K. V. Srinivas, "Downlink resource allocation in multiuser cell-free MIMO networks with user-centric clustering," *IEEE Transactions on Wireless Communications*, vol. 21, no. 3, pp. 1482–1497, 2022.
- [49] B.-Y. Chen, Y.-F. Chen, and S.-M. Tseng, "Hybrid beamforming and data stream allocation algorithms for power minimization in multi-user massive MIMO-OFDM systems," *IEEE Access*, vol. 10, pp. 101 898–101 912, 2022.